In presenting the dissertation as a partial fulfillment of the requirements for an advanced degree from the Georgia Institute of Technology, I agree that the Library of the Institute shall make it available for inspection and circulation in accordance with its regulations governing materials of this type. I agree that permission to copy from, or to publish from, this dissertation may be granted by the professor under whose direction it was written, or, in his absence, by the Dean of the Graduate Division when such copying or publication is solely for scholarly purposes and does not involve potential financial gain. It is understood that any copying from, or publication of, this dissertation which involves potential financial gain will not be allowed without written permission.

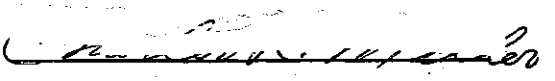

7/25/68

NUCLEAR RELAXATION IN CHLORINATED ETHANES

A THESIS

Presented by

The Faculty of the Division of Graduate

Studies and Research

by

Charles Ralph Miller

In Partial Fulfillment

of the Requirements for the Degree

Doctor of Philosophy

in the School of Chemistry

Georgia Institute of Technology

March, 1970

NUCLEAR RELAXATION IN CHLORINATED ETHANES

Approved by:

Chairman

Date approved by Chairman: 3/17/70

ACKNOWLEDGMENTS

The author wishes to thank the director of this dissertation, Dr. Sidney L. Gordon, for his guidance and encouragement in the accomplishment of this research. He also wishes to express his thanks to the other members of his committee, Dr. Thomas F. Moran and Dr. Ronald H. Felton for their help and suggestions. Mr. Gerald O'Brien designed and built much of the electrical equipment used in this research.

Financial aid from the National Science Foundation in the form of a research assistantship is gratefully acknowledged.

Special thanks are extended to the author's wife, Anne, for her constant encouragement throughout this endeavor.

TABLE OF CONTENTS

		Page
ACKNOWLEDGMENTS		ii
LIST OF TABLES		iv
LIST OF FIGURES		v
SUMMARY		vi
Chapter		
I.	INTRODUCTION	1
	Important Relaxation Mechanisms	1
	Interpretation of Results	2
II.	NUCLEAR RELAXATION THEORY	3
	Spin-Lattice Relaxation	3
	Transverse Relaxation	8
	Calculation of Transition Probabilities	9
	Nuclear Dipole-Dipole Interactions	11
	Scalar Coupling	17
	Other Relaxation Mechanisms	19
III.	RELAXATION TIME MEASUREMENTS	21
	Sample Preparation	21
	T_1 Measurements on A-60D	22
	T_2 Measurements on A-60D	26
	T_1 Measurements on DP-60	30
	Pulse Measurements on DP-60	33
IV.	INTERPRETATION OF DATA	41
	Comparison of Experimental Techniques	41
	1,2-Dichloroethane Study	54
	Dipolar Interactions	57
	Scalar Coupling	66
BIBLIOGRAPHY		69
VITA		72

LIST OF TABLES

Table		Page
1.	Relaxation Times as a Function of Concentration in CS_2. . .	42
2.	Relaxation Times as a Function of Concentration in d_4-1,2-Dichloroethane.	44
3.	Location of Protons Responsible for Spectral Lines Associated with Series of Chlorinated Ethanes	59
4.	Interatomic Distances Associated with Rotational Isomers.	60
5.	Comparison of B.P.P. and Steel Models with Experimental Data.	61
6.	Moments of Inertia.	64
7.	Comparison of Scalar Coupling and Intramolecular Interactions	68

LIST OF FIGURES

Figure		Page
1.	Energy Level Diagram for Two Spin System.	7
2.	Geometrical Quantities Involved in Dipole-Dipole Formulas.	13
3.	An Example of a Recording Used to Determine T_1 on the A-60D	24
4.	An Example of a Recording Used to Determine T_2 on the A-60D	29
5.	An Example of a Recording Used to Determine T_1 by Direct Measurement on the DP-60	32
6.	Block Diagram of Experimental Arrangement for Pulse Measurement	35
7.	Circuit Diagram for rf Power Amplifier.	36
8.	Coupling Circuit for Introducing rf into Probe.	37
9.	$1/T_1$ as a Function of Mole Fraction 1,2-Dichloroethane. . .	45
10.	$1/T_2$ as a Function of Mole Fraction 1,2-Dichloroethane. . .	46
11.	1,2-Dichloroethane in d_4-1,2-Dichloroethane	47
12.	1,2-Dichloroethane in CS_2	48
13.	$1/T_1$ as a Function of Mole Fraction Chloroethane in CS_2 . .	49
14.	Concentration Dependence of $CHCl_2$ Type Protons.	50
15.	Concentration Dependence of CH_2Cl Type Protons.	51
16.	Concentration Dependence of CH_3 Type Protons.	52
17.	Pentachloroethane in CS_2.	53

SUMMARY

The nuclear spin-lattice and transverse relaxation times are measured for the chloroethanes. The measurements are made as a function of concentration in CS_2 and extrapolated to infinite dilution. The spin-lattice relaxation times are obtained from direct observation of the decay curves, and by pulsed NMR techniques. The transverse relaxation times are obtained by adiabatic fast passage. Measurements are made on the Varian DP-60 and A-60D spectrometers. Modifications on the DP-60 are described in detail.

The direct dipolar interactions contribute equally to $1/T_1$ and $1/T_2$. The dipolar interaction between protons on the same carbon provides the major contribution to relaxation. Addition of protons to an adjacent carbon increases the dipolar interaction, but this is usually offset by a decreased correlation time. The proton-chlorine interactions contribute only to the natural line width. These results are then used to establish that the molecular motion of the chloroethanes is controlled more by the moments of inertia of the ethane molecules than by the viscosity of the CS_2 medium.

CHAPTER I

INTRODUCTION

Important Relaxation Mechanisms

The purpose of this thesis is to investigate the nuclear relaxation processes occurring in a series of structurally related compounds. The nuclear spin-lattice and transverse relaxation times of the series of chlorinated ethanes are measured. Meausrements are made as a function of concentration in CS_2 and extrapolated to infinite dilution. Comparisons between different molecules are made at infinite dilution in CS_2. In this way, the behavior of all the molecules is examined in a common medium. This is quite different than previous investigations where the relaxation times of the neat liquid were studied (1,2).

In Chapter II, the relaxation mechanisms are described in detail. The intermolecular dipolar interaction is dependent on the concentration of nuclear moments in the sample and the motional correlation time of the molecule. The intramolecular interaction is proportional to the rotational correlation time and the nature of dipolar interactions within the molecule. Both, intramolecular and intermolecular interactions contribute equally to $1/T_1$ and $1/T_2$. The scalar coupling to a chlorine nucleus is proportional to the chlorine relaxation time. The scalar coupling contributes only to $1/T_2$.

Interpretation of Results

Experimental results are compared to values calculated from the models of Steel (3) and Bloembergen, Purcell, and Pound (4). The B.P.P. model overpredicts $(1/T_1)_{intra}$ by a factor of ten. The Steel model predicts a value that is lower by a factor of two. The comparison indicates that the molecular motion of the chloroethanes is controlled more by the moments of inertia of the molecules than by the viscosity of the CS_2 medium.

The dipolar interaction between protons on the same carbon is much stronger than between protons on adjacent carbons. As protons are added to the same carbon, $(1/T_1)_{intra}$ will increase due to the increased number of dipolar interactions. However, adding protons to an adjacent carbon will usually cause $(1/T_1)_{intra}$ to decrease. The decrease is due to a decrease in rotational correlation time brought about by a decrease in the moment of inertia of the molecule.

CHAPTER II

NUCLEAR RELAXATION THEORY

Spin-Lattice Relaxation

According to the quantum mechanical model of Nuclear Zeeman splitting, a proton with nuclear moment $\underset{\sim}{u}$ in a dc field $\underset{\sim}{H}_o = H_o\hat{k}$ can exist in two spin states. The magnetic quantum number, m, for these states can equal $\pm \frac{1}{2}$, corresponding to the energies $\mp u_z H_o$, respectively. The low energy level corresponds to the nuclear moment $\underset{\sim}{u}$ aligned parallel to $\underset{\sim}{H}_o$; the high energy level corresponds to the anti-parallel orientation. In a macroscopic sample at thermal equilibrium, there will be a slight excess of spins in the low energy level. The ratio of the populations will be given by the Boltzmann factor, $\exp\left(\frac{2u_z H_o}{kT}\right)$. The result is a net component of the magnetization along $\underset{\sim}{H}_o$. The magnetization, $\underset{\sim}{M}$, is the net magnetic moment per unit volume. In order to induce transitions between the two nuclear spin levels, an oscillating electromagnetic field $\underset{\sim}{H}_1 = H_1(\hat{i}\cos\omega t - j\sin\omega t)$ is applied to the system. The rf field has equal probability of producing transitions in both directions. If the number of spins in each energy level were equal, the number of up and down transitions would be equal, and there would be no net absorption of energy from the rf field. However, if the spins are at thermal equilibrium the population of the lower level will slightly exceed that of the upper level by the Boltzmann factor. An absorption of energy will take place corresponding to the transfer

of some of the excess spin population in the lower level to the upper level. If there were no relaxation processes to oppose the effect of the rf field, the population of the levels would become equal, and the absorption of energy would cease. There are, however, relaxation mechanisms which tend to restore the Boltzmann distribution among the spin states by transferring the excess energy to a heat reservoir composed of all of the other degrees of freedom. The other degrees of freedom, when acting as a heat reservoir, are called the lattice. The coupling between the spin system and the lattice is through local fluctuating magnetic fields. The coupling is referred to as spin-lattice interaction and is described by a characteristic time T_1, the spin-lattice relaxation time (4). A strong spin-lattice interaction produces a short relaxation time; a weak interaction produces a long relaxation time.

The spin-lattice relaxation time also measures the time required for the establishment of thermal equilibrium after the application of $\underset{\sim}{H}_o$. Consider an assembly of protons not initially in a magnetic field; then an equal number occupy each of the spin states. Define P_1 as the population of the lower $(+\frac{1}{2})$ state and P_2 as the population of the upper $(-\frac{1}{2})$ state. Let W be the probability per unit time for a given nucleus to make an upward or downward transition by interaction with the lattice. The time rate of population change of each of the nuclear levels can be written as

$$\frac{dP_1}{dt} = -W(P_1-P_1^o) + W(P_2-P_2^o) \qquad (1)$$

$$\frac{dP_2}{dt} = -W(P_2-P_2^o) + W(P_1-P_1^o) \tag{2}$$

where P^o represents the equilibrium population of a particular level. Subtracting Equation (1) from Equation (2) and rearranging terms gives

$$\frac{d(P_1-P_2)}{dt} = -2W(P_1-P_2) + 2W(P_1^o-P_2^o) \tag{3}$$

Since the magnetization along the z axis, M_Z, is proportional to the population difference, Equation (3) may be written as

$$\frac{dM_Z}{dt} = -2W[M_Z(t)-M_Z(\infty)] \tag{4}$$

where $M_Z(\infty)$ is the equilibrium value of $M_Z(t)$. A time T_1 is defined by

$$T_1 = \frac{1}{2W} \tag{5}$$

so that the solution of Equation (4) is

$$M_Z(t) = e^{-t/T_1}[M_Z(0)-M_Z(\infty)] + M_Z(\infty) \tag{6}$$

where $M_Z(0)$ is the initial value of $M_Z(t)$.

In a system of two spins, the time dependent coupling between the spins is capable of inducing transitions between the energy levels

of the combined spin system (7). The two spin system is described by a four level energy diagram as shown in Figure 1. The chemical shift between the two nuclei will be neglected in the following discussion. The resulting simplifications are that energy levels 2 and 3 become degenerate, and that the transition probabilities between levels 1 and 2, 1 and 3, 4 and 2, and 4 and 3 become equal. Also, the transition between levels 2 and 3 is not associated with a transfer of energy to the lattice.

The kinetic equations describing the population changes for the levels of interest are

$$\frac{dP_1}{dt} = -(2W_1+W_2)(P_1-P_1^o) + W_1(P_2-P_2^o) + W(P_3-P_3^o) + W_2(P_4-P_4^o) \qquad (7)$$

$$\frac{dP_4}{dt} = -(2W_1+W_2)(P_4-P_4^o) + W_1(P_2-P_2^o) + W_1(P_3-P_3^o) + W_2(P_1-P_1^o). \qquad (8)$$

The magnetization is

$$M_Z = \frac{Nu_Z}{V}[(P_1)(-1) + (P_2)(0) + (P_3)(0) + (P_4)(+1)] \qquad (9)$$

which reduces to

$$M_Z = Nu_Z(P_4-P_1)/V \qquad (10)$$

where N is the number of molecules contained in a volume V. From Equations (7) and (8)

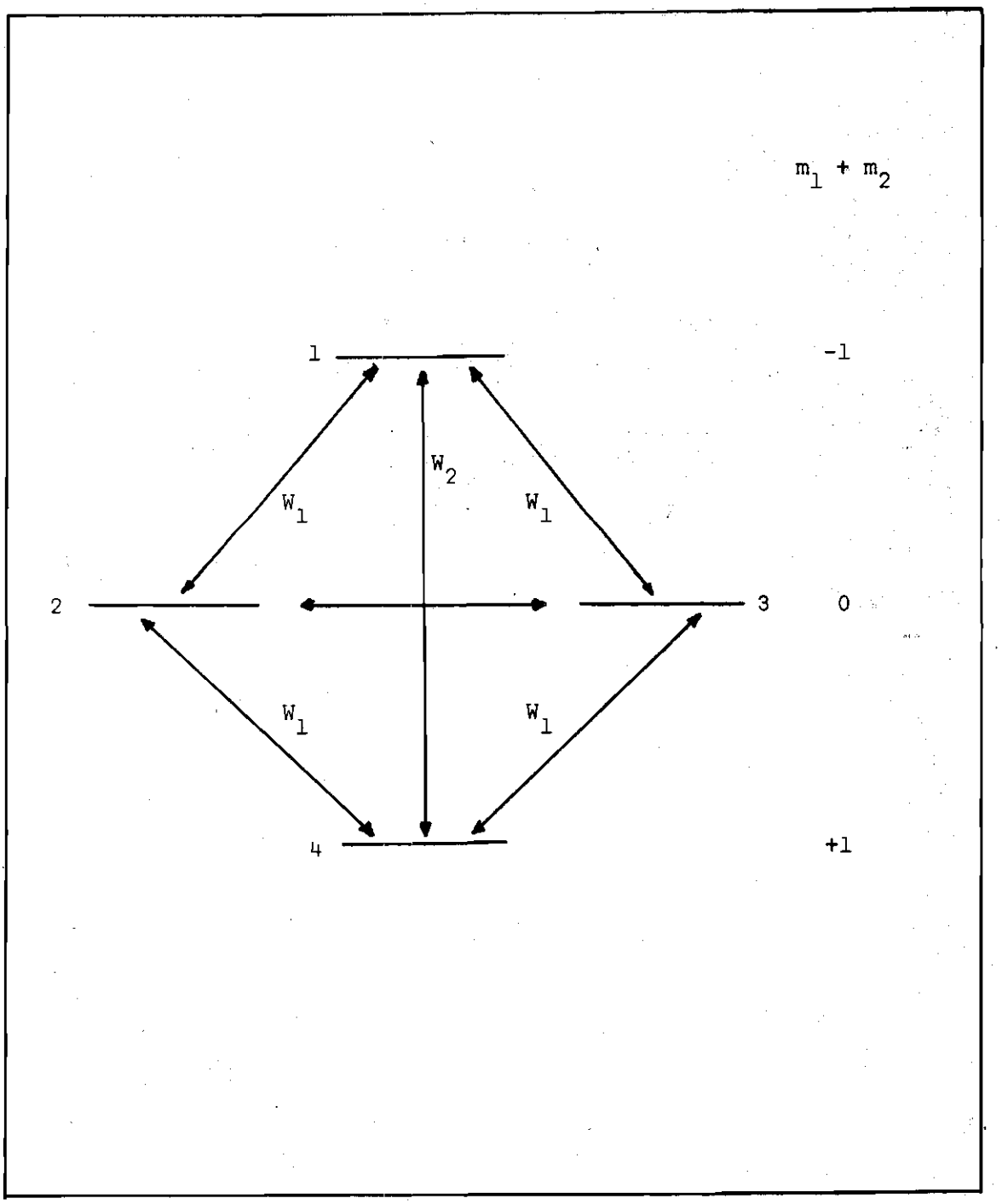

Figure 1. Energy Level Diagram for Two Spin System

$$\frac{d(P_4-P_1)}{dt} = -2(W_1+W_2)[(P_4-P_1) - (P_4^o-P_1^o)]. \qquad (11)$$

Equation (11) can be written in terms of the magnetization as

$$\frac{dM_Z}{dt} = -2(W_1+W_2)[M_Z - M_Z(\infty)]. \qquad (12)$$

In this case

$$(1/T_1) = 2(W_1+W_2) \qquad (13)$$

and

$$M_Z = e^{-t/T_1}[M_Z(0) - M_Z(\infty)] + M_Z(\infty) \qquad (14)$$

which is identical to Equation (6) for a two level system. As can be seen from Equation (5) and Equation (13), any calculation of T_1 requires a knowledge of W.

Transverse Relaxation

As the name implies, transverse relaxation is a relaxation process which destroys the phase coherence introduced by $\underset{\sim}{H}_1$. From a classical viewpoint, the rf field at resonance tends to force the individual nuclear moments to process in phase with each other about $\underset{\sim}{H}_o$. This is because each nucleus sees the same rf field $\underset{\sim}{H}_1$. The result is a component of the magnetization in the XY plane. If the rf field is now turned off the nuclei will lose their phase coherence because the local

molecular fields have no coherence across the sample. The time constant T_2 is the characteristic time in which the assembly of precessing nuclei lose their phase coherence. Therefore, T_2 corresponds to the decay rates of the M_x and M_Y components of the magnetization after $\underset{\sim}{H}_1$ is turned off.

The randomly fluctuating fields that produce the spin-lattice coupling are also responsible for transverse relaxation. Neighboring magnetic moments in the sample cause the individual moments to precess in fields of slightly different strength, hence they precess at different frequencies. In addition, spin-lattice relaxation will affect T_2 because spin transitions will disrupt the phase coherence of the spin assembly. It is not surprising that both T_1 and T_2 are affected by many of the same relaxation mechanisms.

Calculation of Transition Probabilities

According to first-order perturbation theory the probability of a transition in a time t from a state m to a state k, for a single spin, is given by (5)

$$P_{mk}(t) = (1/\hbar^2)\left|\int_0^t H_{mk}(t')e^{-i\omega_{mk}t'}\,dt'\right|^2 \qquad (15)$$

where ω_{mk} is the angular frequency corresponding to the energy difference between the states m and k in the absence of a perturbing random field. In order for Equation (15) to be valid, t must be much less than the relaxation times. It has been shown (5) that the ensemble average of Equation (15) is

$$\langle P_{mk}(t)\rangle_{Av.} = (1/\hbar^2)\left[t \int_{-t}^{t} e^{-i\omega_{mk}\tau} G_{mk}(\tau)d\tau \right. \tag{16}$$

$$\left. - 2 \int_{0}^{t} \cos(\omega_{mk}\tau)\tau G_{mk}(\tau)d\tau \right]$$

where

$$G_{mk}(\tau) = \overline{\langle m|H(t'-\tau)|k\rangle\langle k|\dot{H}(t')|m\rangle} \tag{17}$$

is the correlation function of H(t). A correlation time τ_c is defined as the time τ such that for $\tau > \tau_c$, $G_{mk}(\tau)$ is much smaller than $G_{mk}(0)$. In general, $G_{mk}(\tau)$ approaches zero as τ becomes large. If t can be chosen large compared with the correlation time, yet much less than T_1 and T_2, the second integral in Equation (16) can be neglected compared with the first. The transition probability per unit time becomes independent of t, and is given by

$$W_{mk} = 1/\hbar^2 \int_{-\infty}^{+\infty} G_{mk}(\tau) e^{-i\omega_{mk}\tau} d\tau \tag{18}$$

The fourier transform of $G_{mk}(\tau)$

$$J(\omega_{mk}) = \int_{-\infty}^{+\infty} e^{-i\omega_{mk}\tau} G_{mk}(\tau)d\tau \tag{19}$$

is called the spectral density. The transition probability per unit time can be written in terms of the $J(\omega)$ as

$$W_{mk} = 1/\hbar^2 J(\omega_{mk}) \tag{20}$$

Nuclear Dipole-Dipole Interactions

Among the nuclear interactions responsible for proton relaxation, the dipole-dipole interaction between nuclei is the most important. For the purpose of detailed calculations, it is useful to distinguish between intramolecular dipole-dipole interactions and intermolecular dipole-dipole interactions. The time dependent modulation of the intramolecular dipole-dipole interactions arises exclusively from the rotation of the molecule. In the case of interactions between different molecules, both the relative translations and the molecular rotations should be considered. In order to avoid excessive complication, the rotational effects are neglected when calculating the intermolecular interactions. This introduces an uncertainty into the theoretical interpretation of intermolecular relaxation.

The dipole-dipole interaction between two spins can be written (6)

$$H(t) = \frac{\gamma^2\hbar^2}{r^3}[A+B+C+D+E+F], \tag{21}$$

where

$$A = (1-3\cos^2\theta)I_{1Z}I_{2Z},$$

$$B = -\frac{1}{4}(1-3\cos^2\theta)[I_1^+I_2^- + I_1^-I_2^+],$$

$$C = -\frac{3}{2}\sin\theta\cos\theta e^{-i\phi}[I_{1Z}I_2^+ + I_1^+I_{2Z}],$$

$$D = -\frac{3}{2}\sin\theta\cos\theta e^{+i\phi}[I_{1Z}I_2^- + I_1^-I_{2Z}^2,$$

$$E = -\frac{3}{4}\sin^2\theta e^{-2i\phi}I_1^+I_2^+,$$

and

$$F = -\frac{3}{4}\sin^2\theta e^{+2i\phi}I_1^-I_2^-.$$

The magnetogyric ratio, γ, for a proton is 2.67×10^4 gauss^{-1} sec^{-1}. The angles θ and ϕ are the polar angles defining the direction of the inter proton axis $\underset{\sim}{r}$ with respect to $\underset{\sim}{H}_o$. The geometry is shown in Figure 2. Combining Equations (13) and (20) gives the expression for $1/T_1$ as

$$1/T_1 = (2/\hbar^2)[J(\omega_o) + J(2\omega_o)] \tag{22}$$

where ω_o is the proton Larmor frequency. Therefore,

$$1/T_1 = (2/\hbar^2)\left[\int_{-\infty}^{+\infty} G_{12}(\tau)e^{-i\omega_o\tau}d\tau + \int_{-\infty}^{+\infty} G_{14}(\tau)e^{-i(2\omega_o)\tau}d\tau\right] \tag{23}$$

The intramolecular contribution to $1/T_1$ involves only rotation. It is assumed that the correlation function for the rotation drops off exponentially, and $G(\tau)$ can be approximated by (5)

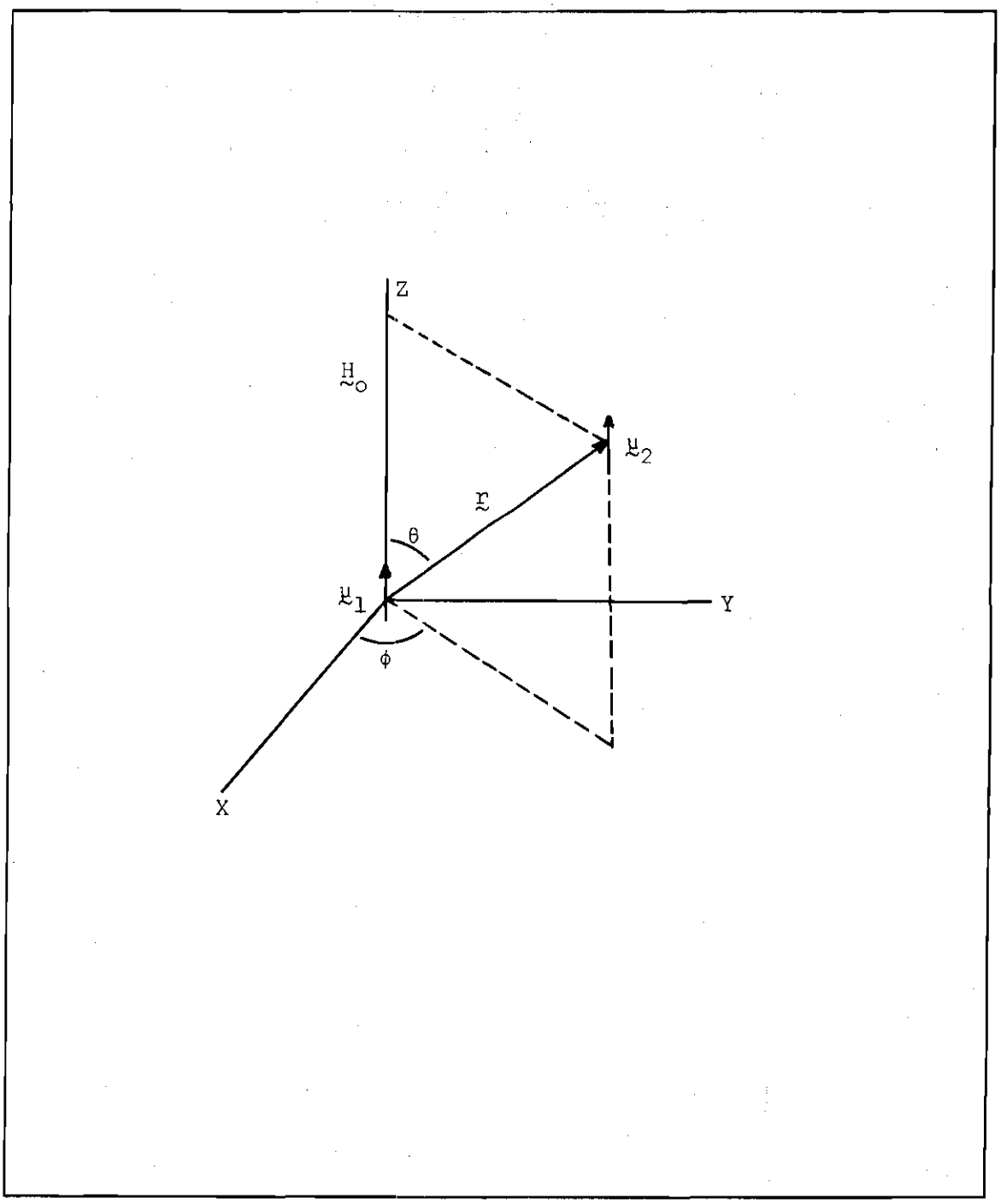

Figure 2. Geometrical Quantities Involved in Dipole-Dipole Formulas

$$G(\tau) = G(0)e^{-|\tau|/\tau_c}. \tag{24}$$

The intramolecular dipole-dipole contribution to $1/T_1$ is found by substituting Equation (24) into Equation (23) and carrying out the integration. Then

$$(1/T_1)_{intra} = (4\tau_c/\hbar^2)\left[\frac{G_{12}(0)}{1+(\omega_o\tau_c)^2} + \frac{G_{14}(0)}{1+(2\omega_o\tau_c)^2}\right]. \tag{25}$$

From Equation (17)

$$G(0) = \overline{|\langle k|H|m\rangle|^2}, \tag{26}$$

and Equation (25) becomes

$$(1/T_1)_{intra} = \frac{4\tau_c}{\hbar^2}\left[\frac{\overline{|\langle 1|H|2\rangle|^2}}{1+(\omega_o\tau_c)^2} + \frac{\overline{|\langle 1|H|4\rangle|^2}}{1+(2\omega_o\tau_c)^2}\right]. \tag{27}$$

where the energy levels refer to Figure 1. The mean square values of the matrix elements in Equation (27) are computed by averaging over all angles (6). They are $(3\gamma^4\hbar^4/20r^6)$ and $(6\gamma^4\hbar^2/20r^6)$ for $\overline{|\langle 1|H|2\rangle|^2}$ and $\overline{|\langle 1|H|4\rangle|^2}$, respectively (6). Using Equation (27)

$$(1/T_1)_{intra} = \frac{3\gamma^4\hbar^2}{10r^6}\left[\frac{\tau_c}{1+\omega_o^2\tau_c^2} + \frac{4\tau_c}{1+4\omega_o^2\tau_c}\right] \tag{28}$$

If $\tau_c\omega_o \ll 1$, extreme narrowing conditions apply, and

$$(1/T_1)_{intra} = \frac{3\gamma^4\hbar^2\tau_c}{2r^6} . \tag{29}$$

It should be recognized that Equation (22) can be generalized to the case where each spin interacts with several spins (7). The equation

$$\frac{dM_Z}{dt} = -(1/T_1)[M_Z(t)-M_Z(\infty)] \tag{30}$$

is still valid with $1/T_1$ for nucleus i given by

$$(1/T_{1i})_{intra} = \frac{2}{\hbar^2}\sum_k [J_{ik}(\omega_o) + J_{ik}(2\omega_o)]. \tag{31}$$

Using Equation (31)

$$(1/T_{1i})_{intra} = \frac{3\gamma^4\hbar^2\tau_c}{2}\sum_k r_{ik}^{-6} . \tag{32}$$

The Debye theory gives

$$\tau_c = 4\pi\eta a^3/3kT \tag{33}$$

where η is the viscosity, and a is the hard sphere radius of the molecule (8). Combining Equation (32) with (33) gives

$$(1/T_{1i})_{intra} = \frac{2\pi\hbar^2\gamma^4\eta a^3}{kT} \sum_k r_{ik}^{-6}. \qquad (34)$$

Gutowsky and Woessner (10) have generalized this expression to include nuclei of a different species. The generalized expression is

$$(1/T_{1i})_{intra} = \frac{2\pi\hbar^2\gamma_i^2\eta a^3}{3kT} \left(3\gamma_i^2 \sum_k r_{ik}^{-6} + 2 \sum_f^* \gamma_f^2 r_{if}^{-6} \right) \qquad (35)$$

where the summations $\sum_k$ are over nuclei of the same species, and $\sum_f^*$ are over all others (9).

The relaxation due to intermolecular dipolar interactions is assumed to arise only from the translational motion of the molecules, the rotation being neglected. The correlation function for the translational motion cannot be described by Equation (24). Bloembergen, Purcell, and Pound (4) have calculated the correlation function by assuming that the translational motion could be described by the classical diffusion equation. The result, generalized by Gutowsky and Woessner to include different nuclei, is

$$(1/T_{1i})_{inter} = \frac{\pi^2\hbar^2\gamma_i^2\eta Na}{kT} \left(3\gamma_i^2 \sum_k \frac{1}{r_{ik}^o} + 2 \sum_f^* \gamma_f^2 / r_{if}^o \right) \qquad (36)$$

which is similar to Equation (35) except that the summations are over nuclei of a neighboring molecule (10). N is the number of molecules per unit volume, and r_{ij}^o is the mean value of r_{ij} for two molecules in

contact. In the crudest approximation, all the r^{o} terms can be replaced by 2a where a, the molecular radius, is estimated from the molar volume.

The total dipole-dipole contribution to $1/T_1$ is given by

$$(1/T_1)_{DD} = (1/T_1)_{intra} + (1/T_1)_{inter}. \qquad (37)$$

The intermolecular term is dependent on the concentration of nuclear moments as is evident from Equation (36). It is possible to evaluate the intramolecular term by extrapolating $(1/T_1)_{DD}$ to infinite dilution in the deuterated analogue. This procedure eliminates the relaxation due to external dipole-dipole interactions, but does not change the physical characteristics of the medium. Such an experiment would yield values for each term in Equation (37).

If the correlation time for the motion responsible for relaxation is very short compared to a Larmor period, i.e., $\omega_o \tau_c << 1$, all the spectral densities become independent of ω, and equal to J(0). The expressions for $1/T_1$ and $1/T_2$ become identical (7). This is the case for dipolar interactions where correlation times are of the order of 10^{-12} sec. If DD represents the dipolar contribution to $1/T_1$ and $1/T_2$, then

$$1/T_1 = 1/T_2 = DD. \qquad (38)$$

Scalar Coupling

Another important relaxation mechanism is the scalar coupling of a spin I to a different spin S that possesses an electric quadrupole

moment. The nuclear spin S has a relatively short relaxation time because of the interaction of its quadrupole moment with the fluctuating electric field gradients. The perturbing Hamiltonian responsible for the relaxation of the spin I is (5)

$$H(t) = hA\underset{\sim}{I}\cdot\underset{\sim}{S}(t) \tag{39}$$

where A is the coupling constant in sec^{-1}. Because of its short relaxation time, the spin S can be assumed to be part of the lattice. The problem then reduces to relaxation in a two level system with $1/T_1$ given by Equation (5). The W is calculated by assuming an exponential correlation function and using Equation (18). The resulting scalar coupling contribution to $1/T_1$ is (7)

$$(1/T_1)_{S.C.} = \frac{2A^2S(S+1)}{3}\left[\frac{T_S}{1 + (\omega_I-\omega_S)^2T_S^2}\right] \tag{40}$$

where ω_I is the Larmor frequency of I, ω_S is the Larmor frequency of S, and T_S is the relaxation time of S. If the spin I is a proton and the spin S a chlorine $(\omega_I-\omega_S)T_S>>1$, and the scalar coupling contribution to $1/T_1$ is negligible.

The transverse relaxation time of the spin I is given by

$$(1/T_2)_I = DD + \frac{A^2S(S+1)}{3}\left[\frac{T_S}{1 + (\omega_I-\omega_S)^2T_S^2} + T_S\right] \tag{41}$$

where the first term DD is the dipolar coupling term and the second term represents the scalar coupling to the chlorine (7). The relaxation time of the chlorine, T_S, is of the order of 10^{-5} sec, and $(\omega_I-\omega_S)T_S>>1$. Equation (41) reduces to

$$(1/T_2)_I = DD + A^2S(S+1)T_S/3. \qquad (42)$$

Other Relaxation Mechanisms

The interaction of nuclear dipoles with the magnetic dipole moments of unpaired electrons could be an important relaxation mechanism. The magnetic moment of the electron is 10^3 times as large as the moment of a nucleus. Therefore, relaxation due to paramagnetic materials could mask the nuclear dipolar interactions, and paramagnetic materials must be removed from the sample. Dissolved atmospheric oxygen is the most common example of a paramagnetic impurity.

In general, the chemical shift depends upon the orientation of the molecule with respect to $\underset{\sim}{H}_o$. Therefore, reorientations due to molecular collisions will produce a fluctuating, shielding field at each nucleus. This mechanism is unique in that it depends on the strength of $\underset{\sim}{H}_o$. In the case of protons, the chemical shifts are small, and the chemical shift anisotropy is not an important relaxation mechanism.

Another possible relaxation mechanism is the interaction of the magnetic field produced by the rotation of the molecule with the magnetic moment of the nucleus. This is known as the spin-rotation interaction and is measured by the spin rotational coupling constant (11).

In the case of a proton, the spin rotation coupling constant is small, and spin rotation is not an important relaxation mechanism (12).

CHAPTER III

RELAXATION TIME MEASUREMENTS

Sample Preparation

Baker reagent grade CS_2 was used exclusively as the solvent. Technical grade 1,1,1-trichloroethane, reagent grade 1,2-dichloroethane and sym-tetrachloroethane were obtained from Fisher Scientific Company. Pentachloroethane, 1,1,1,2-tetrachloroethane and 1,1,2-trichloroethane were obtained from Aldrich Chemical Company. Eastman Kodak practical grade 1,1-dichloroethane was used. The d_4-1,2-dichloroethane was obtained from Merck Sharp and Dohme of Canada Limited. The ethyl chloride was purchased from Matheson.

The oxygen was removed by repeated distillation of the liquid in a vacuum manifold. Before each distillation, some of the material was drawn off with the vacuum pump. The material was then closed off from the system and the system evacuated. The vacuum pump was closed off from the system, and the material was distilled into a bulb cooled by an ice bath. The distillation was repeated at least three times. After the desired number of distillations, the material was distilled directly into an NMR sample tube which was sealed to the vacuum system. The sample tube was then sealed and pulled off the manifold using an oxygen torch.

This method was well suited to the preparation of mixtures of liquids. The liquids were degassed individually, and the desired amount of each was distilled into the NMR sample tube. This technique was best

suited to liquids with relatively low boiling points. The following compounds were degassed by this method: CS_2, 1,2-dichloroethane, 1,1-dichloroethane, 1,1,2-trichloroethane.

An alternative method of degassing is to subject the sample to a series of freeze-pump-thaw cycles. The material to be degassed was placed in the sample tube, and the tube was attached to the vacuum system. The sample was then frozen. The frozen sample was opened to the vacuum system, and the system evacuated. The sample was then closed off from the vacuum system and allowed to thaw. The cycle was repeated at least seven times. This technique was useful for preparing samples with relatively high boiling points. The following compounds were degassed by this method: pentachloroethane, 1,1,1,2-tetrachloroethane, sym-tetrachloroethane.

T_1 Measurements on A-60D

The magnetization of a sample grows to its equilibrium value with a time constant T_1 after the sample is introduced into a dc magnetic field. If the observing rf field H_1 is small enough to avoid appreciable saturation of the spin system, the growth of the ν-mode (absorption mode) signal will follow the rate law

$$S(t) = e^{-(t-t_o)/T_1}[S(t_o)-S(\infty)] + S(\infty) \qquad (43)$$

where t is the time, $S(t_o)$ is the initial value of the signal, and $S(\infty)$ is the equilibrium value.

Another method of determining T_1 is to study the recovery curve obtained after the sample has been saturated by a strong H_1. The spin system is saturated by an rf field when $\gamma H_1 >> (T_1 T_2)^{1/2}$. When the amplitude of H_1 is suddenly reduced to a non saturating value, the recovery of the ν-mode signal will again follow Equation (43). The method of determining T_1 by the growth or recovery of the ν-mode signal is referred to as the direct method.

Direct method measurements were made using the Varian A-60D spectrometer. Time curves were recorded on a Varian G-10 graphic recorder equipped with a 4 in/min chart drive motor. A Hewlett Packard 350D attenuator was connected between the recorder and the A-60D to provide additional control over the signal. The signal was taken from the recorder output jack at the rear of the A-60D.

Measurements were made by sweeping to the center of the resonance line using the slow sweep. The display was adjusted to a convenient height on the G-10 recorder by means of the amplitude control on the A-60D console and the Hewlett Packard attenuator. The sample was then physically removed from the magnetic field for a time equal to at least four relaxation times. At the end of this period, the sample was introduced again into the magnetic field, and the signal recorded as a function of time. It is essential that the magnetic field is sufficiently inhomogeneous, otherwise the line will be too narrow. For narrow lines it is difficult to keep the recorder on top of the peak. A slight drift of the main magnetic field will move the spectrometer away from the resonance condition causing a decrease in signal intensity. For this

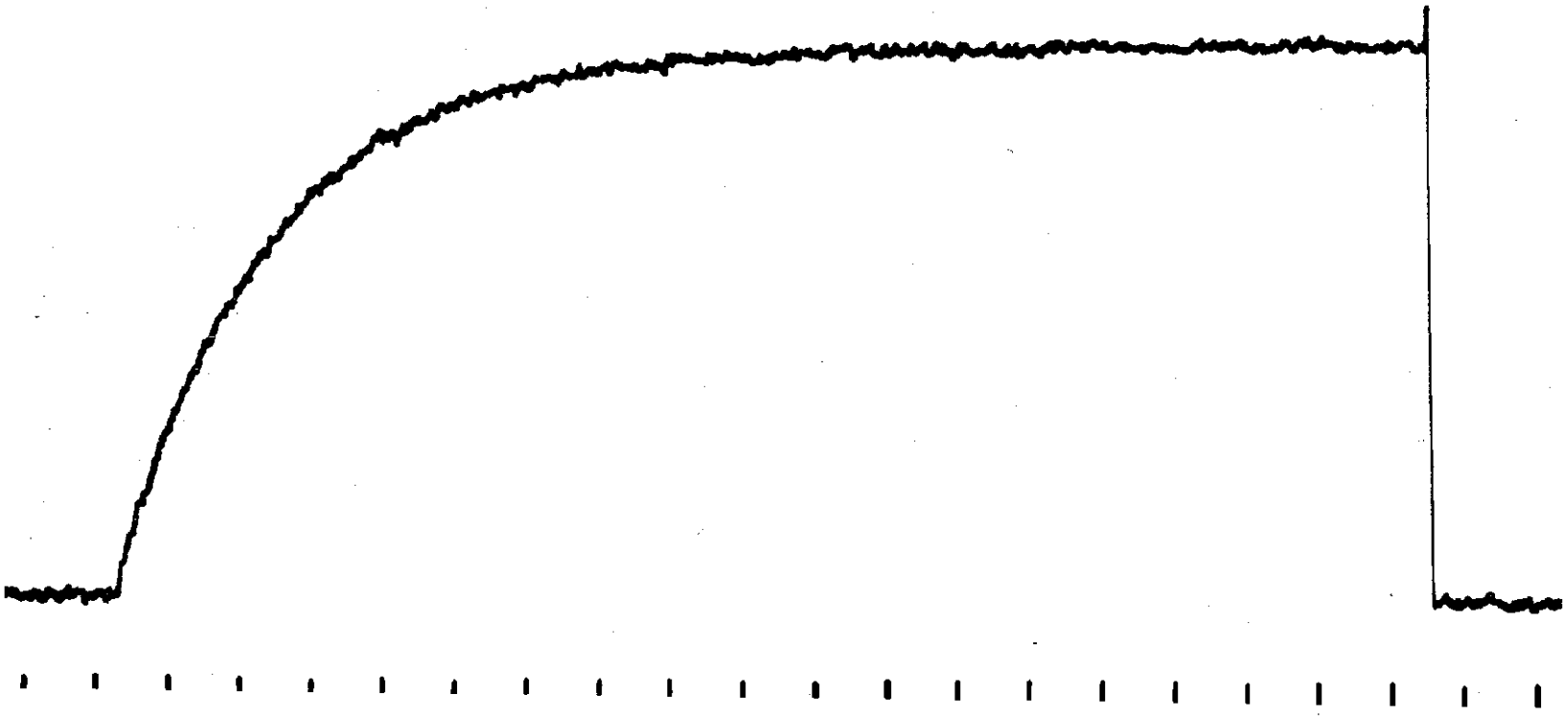

Figure 3. An Example of a Recording Used to Determine T_1. The Sample is 80 Volume Per Cent 1,1,1-Trichloroethane in CS_2. The Time Markers Occur at Six-Second Intervals

reason the line was purposely broadened by about 30 cps. This was conveniently done by not spinning the sample. Additional line broadening may be accomplished by offsetting the Y-gradient fine control.

Figure 3 is a typical recorder trace obtained by the direct method. The chart speed was calibrated so that time could be read directly from the chart. The decay was assumed to be exponential and to follow Equation (43). A plot of log $\left[\frac{S(\infty)-S(t)}{S(\infty)-S(t)}\right]$ against $(t-t_o)$ gave a straight line with a slope given by

$$\text{Slope} = 1/(2.303)(T_1). \tag{44}$$

Data was treated by the method of least squares and fit to $Y = mx + c$. A data point which varied more than 2.5 times the standard deviation was rejected. New slope and intercept constants were calculated until all deviations were less than the prescribed limit. The calculations were programmed in Algol for the Burroughs B-5500.

The direct method has the advantages of simplicity and a straightforward interpretation of the experiment. It can be used with most NMR spectrometers and requires little or no modification of the spectrometer. With the direct method, the relaxation time of individual chemically shifted lines of the NMR spectrum can be determined. The method is applicable to relaxation times between 1 second and 40 seconds. The 1 second lower limit is due to the essential requirement that all circuit time constants be short enough to follow the increase in the NMR signal. For times above 40 seconds, saturation effects

artificially lower the relaxation time. The sensitivity of the direct method is limited by the steady state nature of the experiment and is not as great as can be achieved by transient methods.

T_2 Measurements on A-60D

The method used for measuring T_2 was to observe the decay of the transverse magnetization in the presence of a strong rf field (25). The magnetization is turned into a plane perpendicular to the main field by doing an adiabatic rapid passage into the center of the resonance line (13). In order for an adiabatic rapid passage to occur, the inequalities

$$1/T_2 << \frac{1}{H_1}\left|\frac{dH_o}{dt}\right| << \gamma H_1 \qquad (45)$$

must be satisfied (14). Under these conditions, the magnetization remains aligned along $\underset{\sim}{H}_{eff} = \left(H_o - \frac{\omega}{\gamma}\right)\hat{k} + H_1\hat{i}$. At resonance H_{eff} is parallel to H_1. Since γH_1 is large compared to $1/T_1$, the magnetization will maintain its position along H_1. However, the magnitude of the magnetization will decay with a time constant to be denoted by $T(H_1)$. $T(H_1)$ is not necessarily equal to T_2 because $T(H_1)$ is the decay constant observed in the presence of the rf field, whereas T_2 characterizes the decay in the absence of H_1 (15).

It has been shown for a system whose relaxation is caused, in part, by slow motions such as chemical exchange or scalar coupling that

$$1/T(H_1) = K\tau_c/(1+\omega_1^2\tau_c^2) + 1/T_1 \qquad (46)$$

where K contains the constants of the slow relaxation mechanism and $1/T_1$ is the contribution from mechanisms involving short correlation times. In the limit $\omega_1 \rightarrow 0$, Equation (46) reduces to $1/T_2$. Thus, T_2 can be obtained by measuring $1/T(H_1)$ as a function of H_1 and extrapolating to $\omega_1 = 0$.

T_2 for 1,2-dichloroethane was measured at field strengths from 0.3 to 10 milligauss. T_2 was found constant over this range, indicating that $\gamma H_1 \tau_c << 1$ for these samples. Therefore, extrapolation to $\omega = 0$ was not necessary.

The Varian A-60D Spectrometer equipped with a Varian V-5058A spin decoupler was used for the T_2 measurement. A Varian G-10 recorder and a Hewlett Packard 350D attenuator were used as described for the direct method experiments.

The spin decoupler was set to the "HI FIELD H_1" position. H_1 and a field sweep rate were chosen such that the adiabatic conditions of Equation (45) apply. In addition, the magnitude of H_1 was made large compared to the inhomogeneties of the applied magnetic field across the sample. A simple check on the conditions chosen was performed by observing the signal on the A-60D recorder as the field was swept through resonance. If the conditions for adiabatic fast passage were met, the line was inverted when sweeping from a low to a high field. After several T_1's, sweeping back through resonance from a high to a low field produced an upright line.

Measurements were accomplished by sweeping to the center of the resonance line and stopping the sweep. The center of the resonance

line is indicated by a maximum μ-mode (dispersion mode) signal. The decay of the signal from a maximum value was recorded on the G-10 recorder as a function of time. After the signal had reached its limiting value of zero, the field was swept away from the resonance condition. An example of a recorder trace used to determine T_2 is given in Figure 4. The effect of stopping the sweep either below or above resonance has been discussed by Bonera *et al.* (13). The chart speed was calibrated and the time read directly from the chart. The decay was exponential and of the form of Equation (43). Data was treated in a manner identical to that described for the direct method measurement of the spin-lattice relaxation time.

The adiabatic fast passage method of measuring T_2 is applicable to a large class of interesting materials, i.e., many organic liquids. Transverse relaxation times between 5 seconds and 40 seconds can be measured by this method. The lower limit of applicability of the method is due to the requirement that all circuit time constants be short enough to follow the change in the signal intensity. The upper limit is set by the ability of the spectrometer's lock system to compensate for drift in the magnetic field. Measurements can be performed on the A-60D without modification that would affect the use of the spectrometer as a routine analytical tool. The method of adiabatic fast passage has several advantages over the more commonly used pulse techniques for the measurement of T_2. The Carr-Purcell method of spin echoes is excellent for T_2 less than one second, but becomes less useful for longer values of T_2 because of extreme stability requirements on the pulse train. The

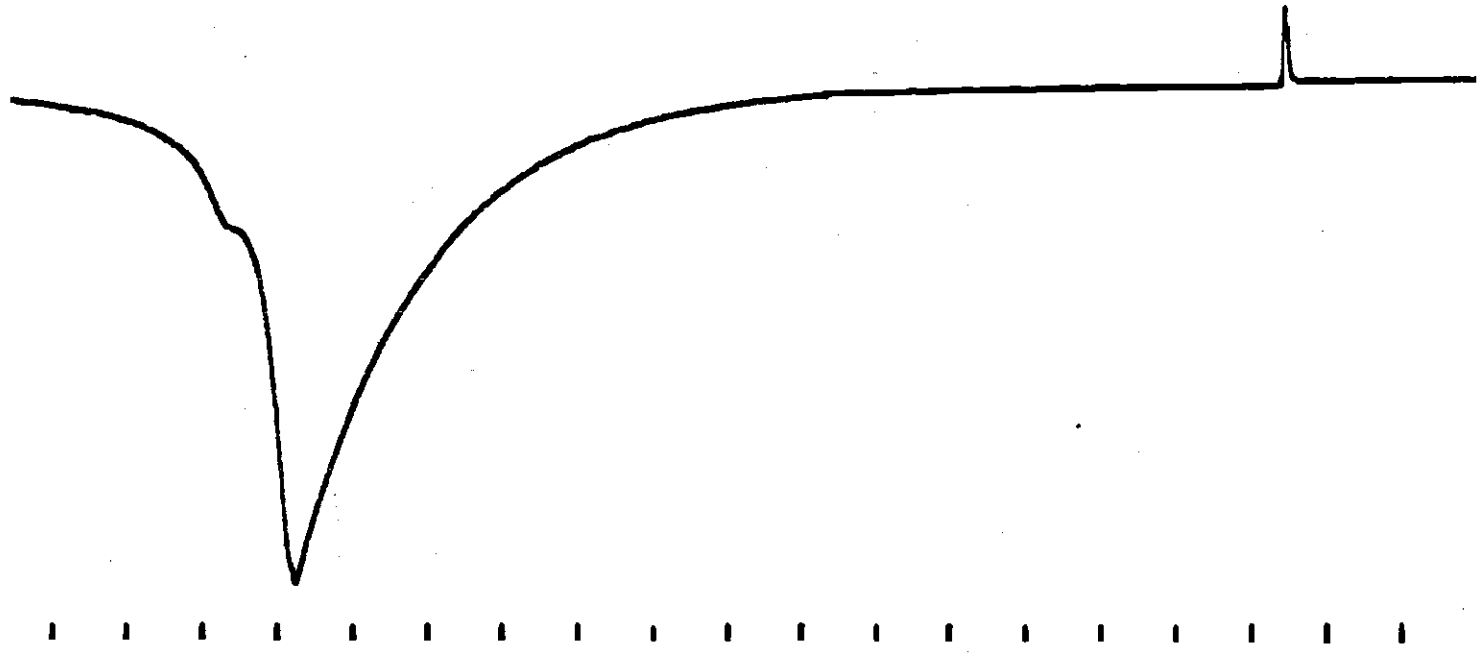

Figure 4. An Example of a Recording Used to Determine T_2. The Sample is 80 Volume Per Cent 1,1,1-Trichloroethane in CS_2. The Time Markers Occur at Six-Second Intervals

method of adiabatic fast passage also allows measurement of T_2 on individual chemically shifted lines rather than simply a T_2 for the whole molecule as is often the case in pulse measurements.

T_1 Measurements on DP-60

A variation of the direct method of measuring T_1 involves the reversal of the magnetization by means of an adiabatic rapid passage. The magnetization can then be monitored periodically with a weak rf field. The time dependence of the v-mode signal will follow Equation (43).

Measurements were made using the Varian DP-60 spectrometer and an audio phase sensitive detector of the type described by Noggle (16). The signal from output No. J314 of the V4311 rf detector was supplied to the stabilizer section of the spin decoupler (phase sensitive detector No. 1) described in reference 12. The dc output of the phase detector was displayed on a Varian G-10 recorder. A Hewlett Packard 200CDR oscillator supplied the additional audio-frequency modulation necessary to produce an adiabatic reversal of the magnetization.

The magnetic field was modulated at 1 kc/sec on the NMR spectrum detected at 60 Mc/sec. All measurements were performed on the low field sideband. The V4311 unit was operated at 20db attenuation and a receiver gain of two. The modulation level and signal level were adjusted at the spin decoupler to provide an adequate signal-to-noise ratio. The Hewlett Packard 200CDR oscillator was adjusted for a 1 kc/sec output. During one sweep through resonance, the 200CDR was connected to the field modulation input on the V4352 unit. The increased

modulation allowed more rf power to enter at the sideband frequency so that the adiabatic conditions applied. The magnetization was then monitored periodically with the low rf, i.e., the 200CDR was disconnected. The sampling period was determined by the sweep rate controls on the V4352 fast sweep unit. Figure 5 shows a recording of the signals from the doublet in a sample of 80 volume per cent 1,1,2-trichloroethane in CS_2.

Data was treated in a manner identical to that described for the direct method measurement of the spin-lattice relaxation times on the A-60D. The V4352 sweep rate was calibrated and, the peaks in Figure 5 occur at 4.00 sec intervals. The peak heights were assumed to measure the signal, S(t), of Equation (43).

As with the direct method on the A-60D, this technique also allows measurements to be performed on individual chemically shifted lines. Since the magnetization is sampled by sweeping over the line rather than by sitting on the line, saturation effects are not nearly as large. Therefore, longer T_1's can be measured than are accessible on the A-60D. Relaxation times between 10 and 100 seconds can be measured. The lower limit is again due to circuit time constants. The upper limit is governed by the signal-to-noise ratio, and the necessity of avoiding saturation of the spin system by the observing rf field. The method eliminates the problem of drift inherent in the direct method experiment on the A-60D. A small drift will not affect the results and a large drift can be compensated for by observing the side band resonance signal on an oscilloscope and applying a field correction with

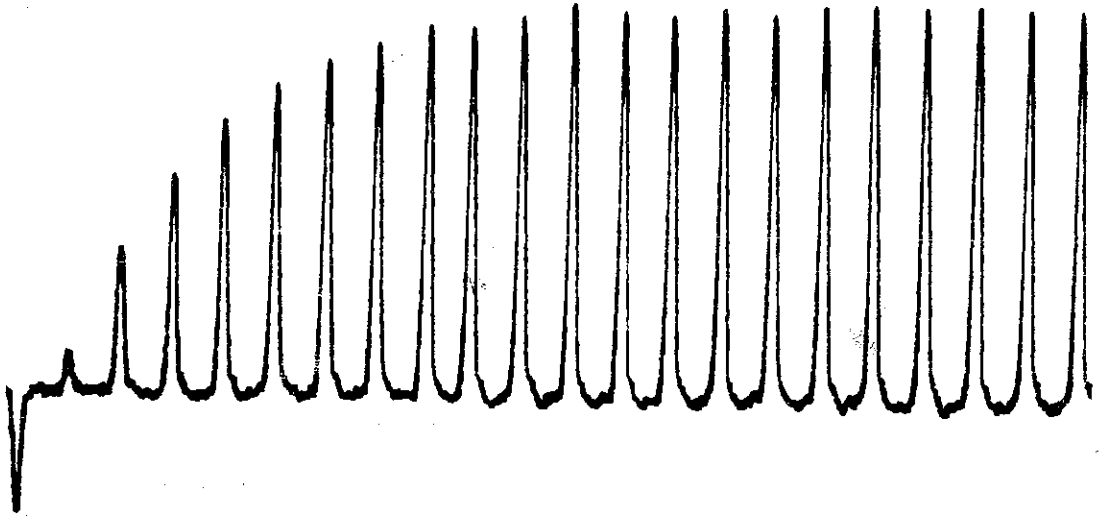

Figure 5. An Example of a Recording Used to Determine T_1 by Direct Method Measurements on the DP-60

the V3507 slow sweep and drift controls. Since the growth of the signal begins from a negative value for the inverted magnetization, a larger number of data points are available.

Pulse Measurements on DP-60

A pulse of rf energy at the resonance frequency rotates the magnetization away from its equilibrium direction along the main magnetic field (17). The magnetization rotates with an angular velocity γH_1, where H_1 is the amplitude of the rf field. If the rf field is turned on for a time interval of t seconds, the magnetization will rotate through an angle of $\gamma H_1 t$ radians. If H_1 and t are chosen such that $\gamma H_1 t = \pi/2$, the magnetization will be turned into a plane perpendicular to the main field. Such pulses are referred to as $\pi/2$ pulses. Pulses for which $\gamma H_1 t = \pi$ are π pulses, and have the effect of reversing the direction of the magnetization (18). In practice H_1 is made large and the duration of the pulse made short so that relaxation effects are negligible during the pulse.

The spin-lattice relaxation time was measured by applying a π pulse followed by a $\pi/2$ pulse at some later time. The π pulse sets the initial conditions for the experiment by inverting the magnetization. The magnetization would then recover its equilibrium value with a time constant T_1. A $\pi/2$ pulse applied during the recovery caused the magnetization to rotate into a plane perpendicular to the main field. The signal produced by the $\pi/2$ pulse was proportional to the magnetization at the time of the pulse. The $\pi/2$ response was taken as a measure of the S(t) in Equation (43).

Measurements were made at 60Mc/sec using a Varian DP-60 NMR spectrometer which was modified in a manner similar to that described by Meiboom (19). The pulse system consisted of two Tektronix 160 series pulse generators, a Tektronix type 162 waveform generator and a type 160A power supply. A Tektronex type 360 indicator was used for observing the output of the pulse generators. The pulse system was similar to that used by Meiboom. A block diagram of the experimental arrangement is shown in Figure 6. The transmitter section of the V4311 unit was modified so that it could be gated on using negative signals from the Tektronex 160 series pulse generators. The transmitter modification was described by Meiboom (19). The Meiboom modification of the receiver section of the V4311 unit was not used. The output of the V4311 transmitter was amplified by a tuneable rf power amplifier with a power gain of 40db. A schematic diagram of the amplifier is given in Figure 7. The probe was modified by removing the variable capacitor from the transmitter input section. A coupling circuit shown in Figure 8 was used to replace the capacitor. The output of the rf power amplifier was applied to the coupling circuit and the coupling circuit output applied directly into the transmitter coil. The two variable capacitors in the coupling circuit were tuned to match the impedance of the rf amplifier and optimize the power transfer to the transmitter coil. The time interval between the π and $\pi/2$ pulses was measured with a Hewlett Packard 5245L electronic counter equipped with a 5262A time interval unit. The V4311 receiver output was recorded on a Tektronix type 564B storage oscilloscope. A block diagram of the experimental arrangement is shown in Figure 6.

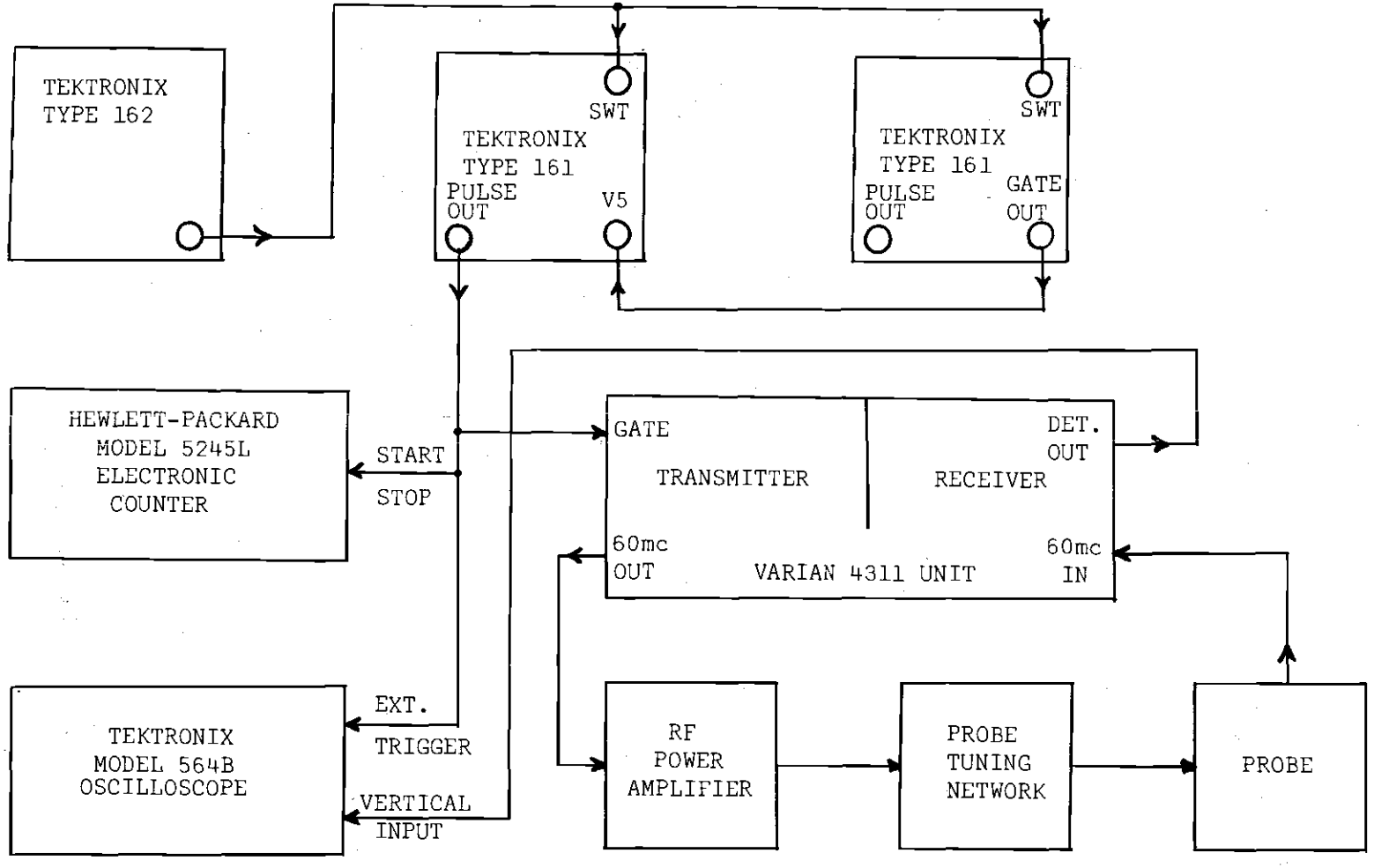

Figure 6. Block Diagram of Experimental Arrangement for Pulse Measurement

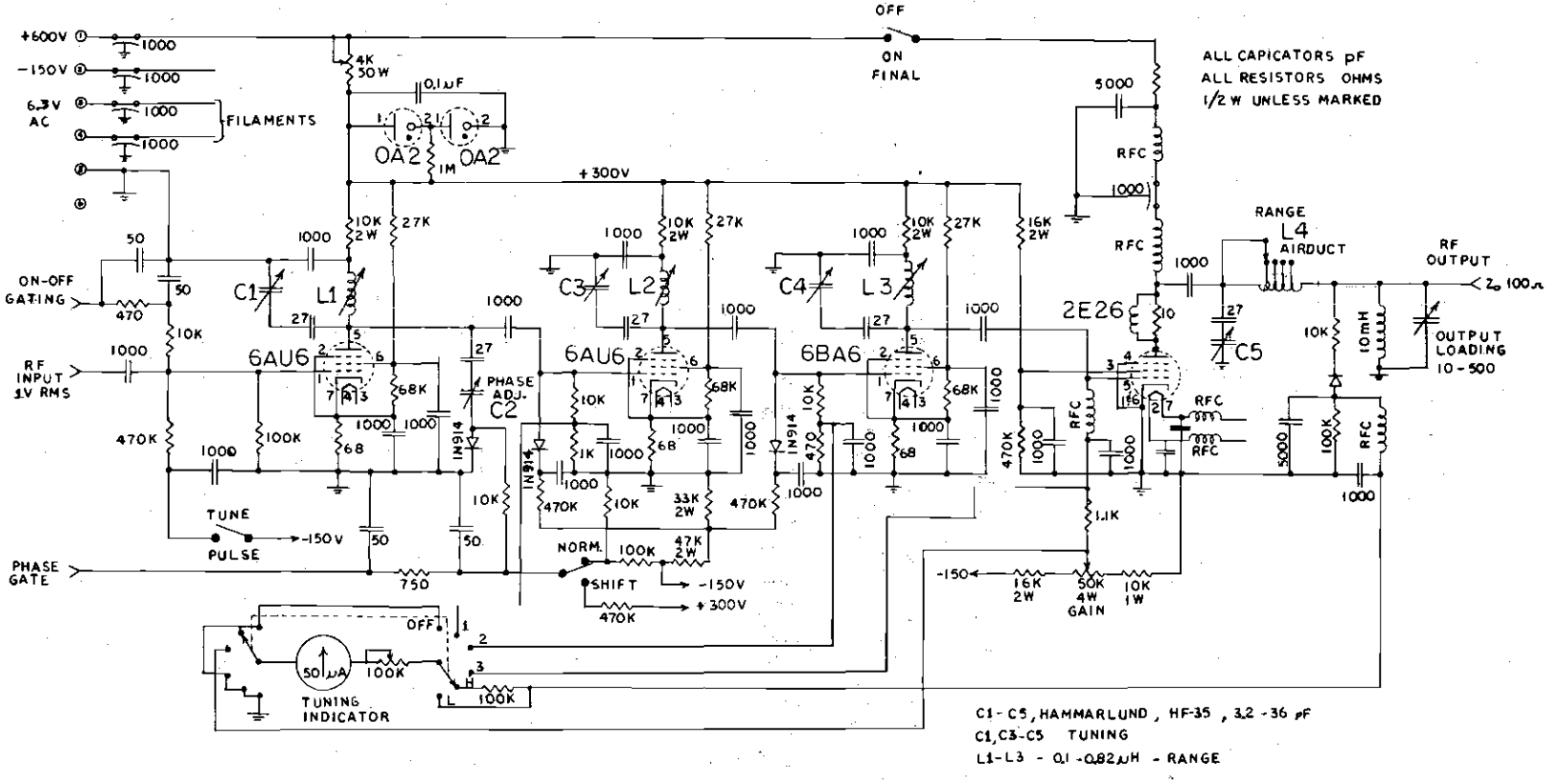

Figure 7. Circuit Diagram of rf Power Amplifier

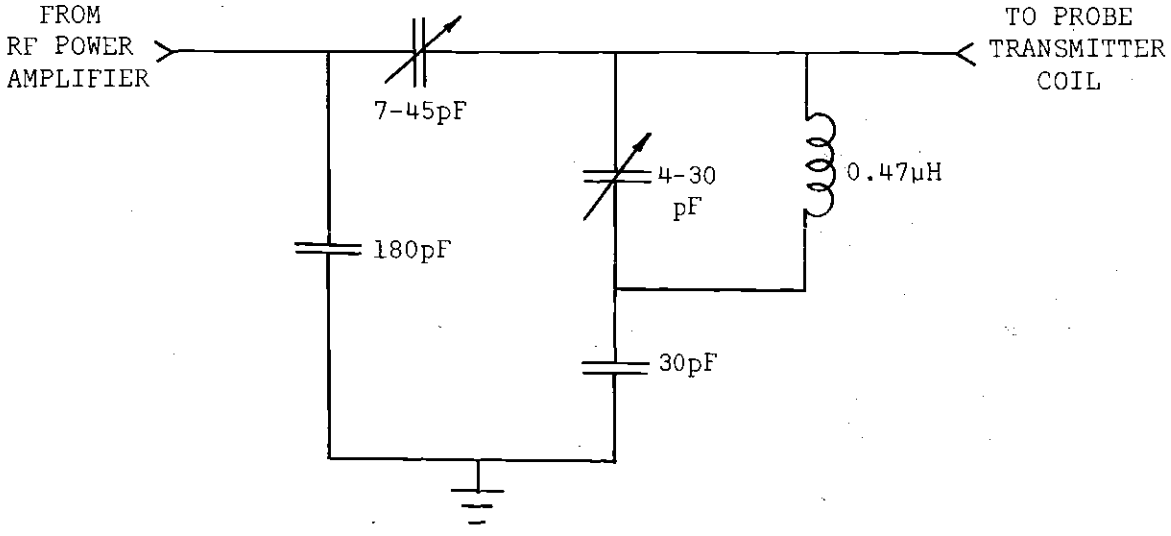

Figure 8. Coupling Circuit for Introducing rf into Probe

Measurements were made by observing the beat pattern produced by phase detection the free induction signal at the V4311 reference frequency. The magnetic field, $\underset{\sim}{H}_o$, was adjusted so that $\gamma H_o/2\pi$ was 200 cps from the V4311 unit frequency. The 200 cps beat pattern was displayed on the storage oscilloscope at a 5 msec/div sweep rate so that the beat oscillations were clearly visible. The difference between $\gamma H_o/2\pi$ and the V4311 frequency was always readily known by the frequency of the beat pattern. The 200 cps position was maintained by applying a field correction with the V3507 slow sweep and drift controls. The amplitude of a convenient oscillation in the beat pattern was assumed to be proportional to the magnetization. The V4311 receiver was momentarily saturated by leakage during each pulse. The recovery time of the receiver was less than 10 msec. Therefore, the oscillation measured was chosen to occur 10 msec after the end of the π pulse. The time in Equation (43) is the time interval between the π and $\pi/2$ pulses.

The pulse generators were adjusted so that one produced a $\pi/2$ pulse and the other a π pulse. This was conveniently accomplished with a water sample whose line width was artificially broadened to 8 cps by addition of paramagnetic material. The response to the pulse was observed to pass through a maximum as the pulse duration was increased. That pulse duration which produces the maximum response is a $\pi/2$ pulse. If the pulse duration was increased further, the amplitude went through a minimum. The pulse producing the minimum was a π pulse. The duration of the π pulse was approximately twice that of the $\pi/2$ pulse. The π pulse used for T_1 measurements had a duration of 0.35 msec, indicating an rf field strength of 1400 cps.

The sample was placed in the probe, and several relaxation times were allowed to pass. The sample was then subjected to the $\pi - \pi/2$ pulse sequence. As soon as the response to the π pulse appeared on the oscilloscope, the field was corrected to the 200 cps from resonance position. The π pulse was erased from the oscilloscope in anticipation of the $\pi/2$ pulse response. The π pulse was used to start the electronic counter, and the $\pi/2$ pulse to stop it. The time interval between pulses was read directly from the counter. Next, the time interval between the pulses was changed, and after waiting several relaxation times, the experiment was repeated. This procedure was continued until the desired number of data points had been collected. The equilibrium value of the signal was determined by an average of at least three measurements. The equilibrium signal is the response to a single $\pi/2$ pulse. A period of several relaxation times must precede each determination of the equilibrium amplitude.

The free induction signal will saturate the V4311 receiver if it is too large. The V4311 unit was designed for amplification of much weaker steady state signals. Receiver saturation was eliminated by keeping the final output of the V4311 receiver below 0.50 volts when responding to a $\pi/2$ pulse. The receiver was operated in the lowest gain position, and the input signal to the receiver was reduced by detuning the coupling capacitor in the receiver section of the probe. Saturation of the receiver produces artificially shortened time constants.

Data was treated by a graphical method. A plot of log $\left[1 - \frac{S(t)}{S(\infty)}\right]$ against time gave a straight line with a slope given by

$$\text{Slope} = -1/2.303T_1. \tag{47}$$

At least seven data points were used for each determination.

The pulse method is the most accurate method for measuring T_1. The serious problem of saturation, which limits the direct methods, does not occur in the pulse technique. Relaxation times as long as three minutes have been measured. The upper limit is set by the signal-to-noise ratio and magnetic field drift. A T_1 of 70 msec was measured for a doped water sample with the apparatus described. Smaller T_1's are readily accessible with an increase in rf power. The pulse method, as described, is not applicable to compounds possessing more than one line in their NMR spectrum.

CHAPTER IV

INTERPRETATION OF DATA

Comparison of Experimental Techniques

Wherever possible, more than one experimental technique was used to measure T_1's. This provided a test of the validity of the various T_1 measuring techniques used in this investigation. It was also useful in determining which technique was best suited for a particular range of T_1's. Unfortunately, only one technique, the adiabatic fast passage method, was suitable for measuring the T_2's.

The pulse method was the most reliable because of the absence of saturation effects. The pulse method data in Tables 1 and 2 is the result of only one measurement. An estimate of the error in this experiment was made by performing three measurements on a sample of 20 per cent 1,2-dichloroethane in CS_2. The average deviation of the three measurements was 5 per cent. The pulse method was applied to all compounds exhibiting one line spectra. The dilution plots in Figures 9 through 17 for one line compounds were constructed from the pulse data in Tables 1 and 2. The A-60D data for the one line compounds is used only for comparison of experimental techniques.

The direct method on the A-60D is applicable to measurement of relaxation times up to about 40 sec. Both lines in the ethyl chloride spectrum as well as the doublets in 1,1-dichloroethane and 1,1,2-trichloroethane were measured on the A-60D. The values from DP-60

Table 1. Relaxation Times as a Function of Concentration in CS_2

Volume %	T_2, Sec	T_1 Sec(Pulse)	T_1 Sec(A-60D)
1,1,1-Trichloroethane			
Neat	10.39±0.032	10.40	10.24±0.25
80	11.46±0.18	12.30	11.83±0.17
60	11.83±0.05	13.00	13.52±0.48
40	12.43±0.12	-	-
20	12.61±0.30	14.90	14.68±0.98
Sym-Tetrachloroethane			
Neat	18.50±0.62	21.20	
80	22.20±0.63	29.80	
60	26.46±0.18	43.50	
40	29.50±0.44	50.07	
20	29.78±1.95	63.40	
1,2-Dichloroethane			
Neat	10.61±0.31	11.50	11.22±0.36
80	12.45±0.08	13.85	14.83±1.19
60	14.20±0.39	16.70	16.28±0.27
40	16.48±0.23	21.00	19.62±0.97
20	18.12±0.02	26.50	23.88±0.36
1,1,1,2-Tetrachloroethane			
Neat	9.10±0.14	9.05	8.60±0.05
80	11.49±0.36	12.20	11.68±0.34
60	13.75±0.06	15.20	14.66±0.59
40	15.13±0.34	16.90	16.94±0.72
20	16.60±0.12	20.30	20.11±1.35
Pentachloroethane			
Neat	33.41±0.32	43.50	
80	42.05±0.20	91.30	
60	44.83±1.80	126.09	
40	47.73±2.60	160.13	
20	-	186	

Table 1. Continued

Volume %	T_2, Sec	T_1 Sec(A-60D)	T_1 Sec(DP-60)
1,1-Dichloroethane(Doublet)			
Neat	9.30±0.27	10.40±0.25	10.60±0.08
80	10.98±0.29	12.37±0.04	11.88±0.32
60	11.59±0.11	13.19±0.11	13.02±0.50
40	11.74±0.25	14.11±0.24	14.43±0.25
20	12.09±0.26	15.23±0.15	14.88±0.10
1,1-Dichloroethane(Quartet)			
Neat	12.90±0.38		25.58±1.05
80	15.94±0.49		37.75±1.33
60	16.48±0.09		47.87±0.14
40	16.70±0.38		63.79±2.03
20	18.35±0.35		74.02±2.53
1,1,2-Trichloroethane(Doublet)			
Neat	8.38±0.02	8.18±0.40	8.32±0.26
80	10.71±0.04	10.75±0.15	10.70±0.30
60	11.93±0.30	13.41±0.15	13.87±0.34
40	14.43±0.38	15.58±0.16	15.00±0.20
20	16.44±0.35	18.75±0.70	21.00±0.32
1,1,2-Trichloroethane(Triplet)			
Neat	15.62±0.21		23.97±0.16
80	20.85±0.35		32.54±0.86
60	22.60±0.14		42.79±0.44
40	28.39±0.48		61.00±0.34
20	28.96±0.26		68.12±1.22
Ethyl Chloride(Quartet)			
Neat	13.37±0.18	25.86±0.48	
80	15.18±0.58	29.13±0.74	
60	15.93±0.17	27.87±1.56	
40	16.86±0.50	33.15±1.17	
30	-	31.63±0.41	
20	16.98±0.39	36.91±1.53	

Table 1. Continued

Volume %	T_2, Sec	T_1 Sec(A-60D)	T_1 Sec(DP-60)
Ethyl Chloride(Triplet)			
Neat	11.76±0.13	20.86±0.40	
80	12.63±0.88	21.11±0.51	
60	13.53±0.53	22.37±0.55	
40	13.50±0.31	25.08±0.90	
30	-	26.82±0.37	
20	14.88±0.53	28.38±1.07	

Table 2. Relaxation Times of 1,2-Dichloroethane as a Function of Concentration in d_4-1,2-Dichloroethane

Volume %	T_2, Sec	T_1, Sec(Pulse)
Neat	10.61±0.33	11.50
90	-	12.00
80	11.19±0.07	12.00
60	11.63±0.27	13.23
50	-	14.20
40	13.14±0.22	14.68
20	-	16.00
15	14.53±0.36	-
10	-	16.00

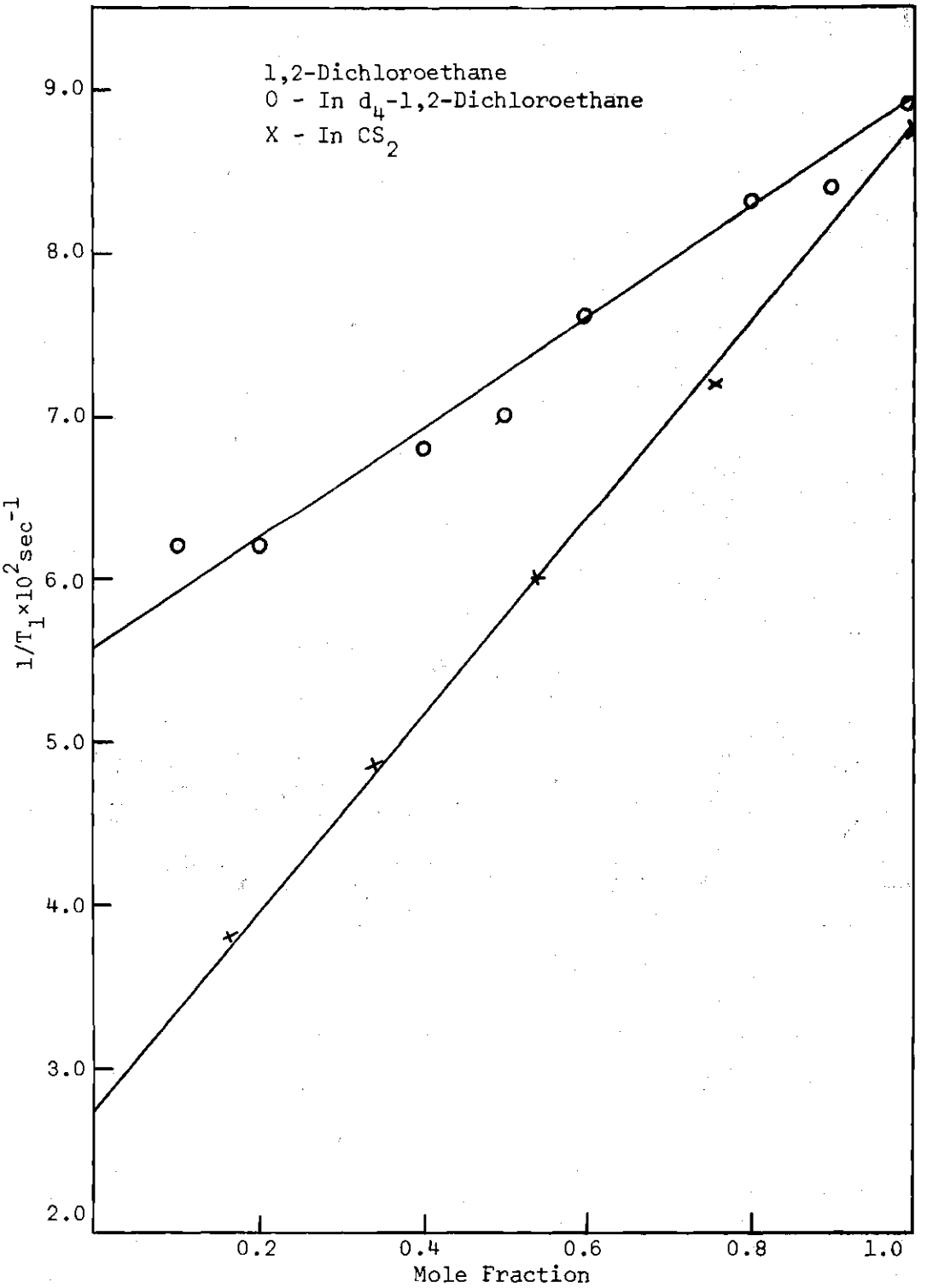

Figure 9. $1/T_1$ as a Function of Mole Fraction 1,2-Dichloroethane

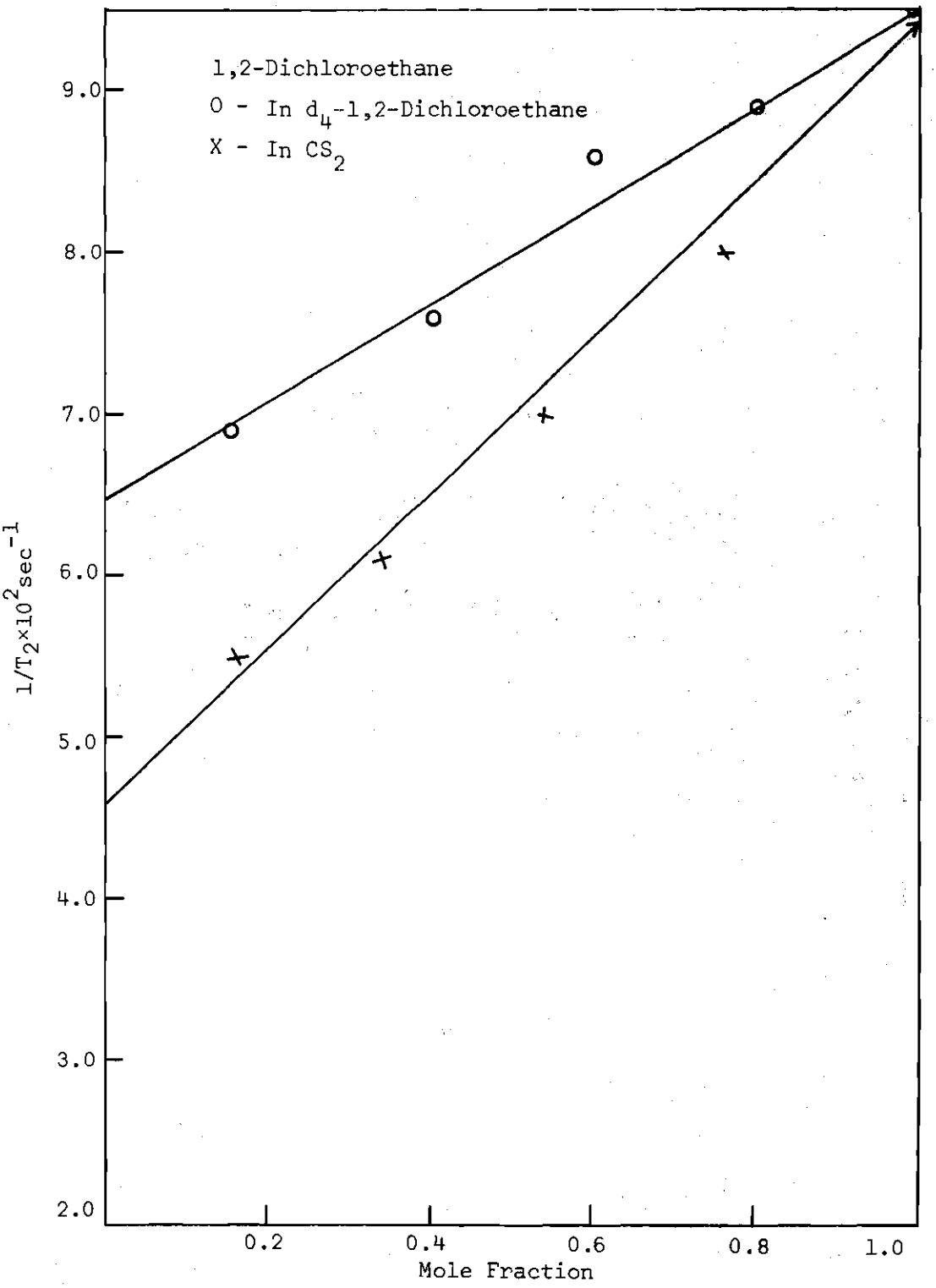

Figure 10. $1/T_2$ as a Function Mole Fraction 1,2-Dichloroethane

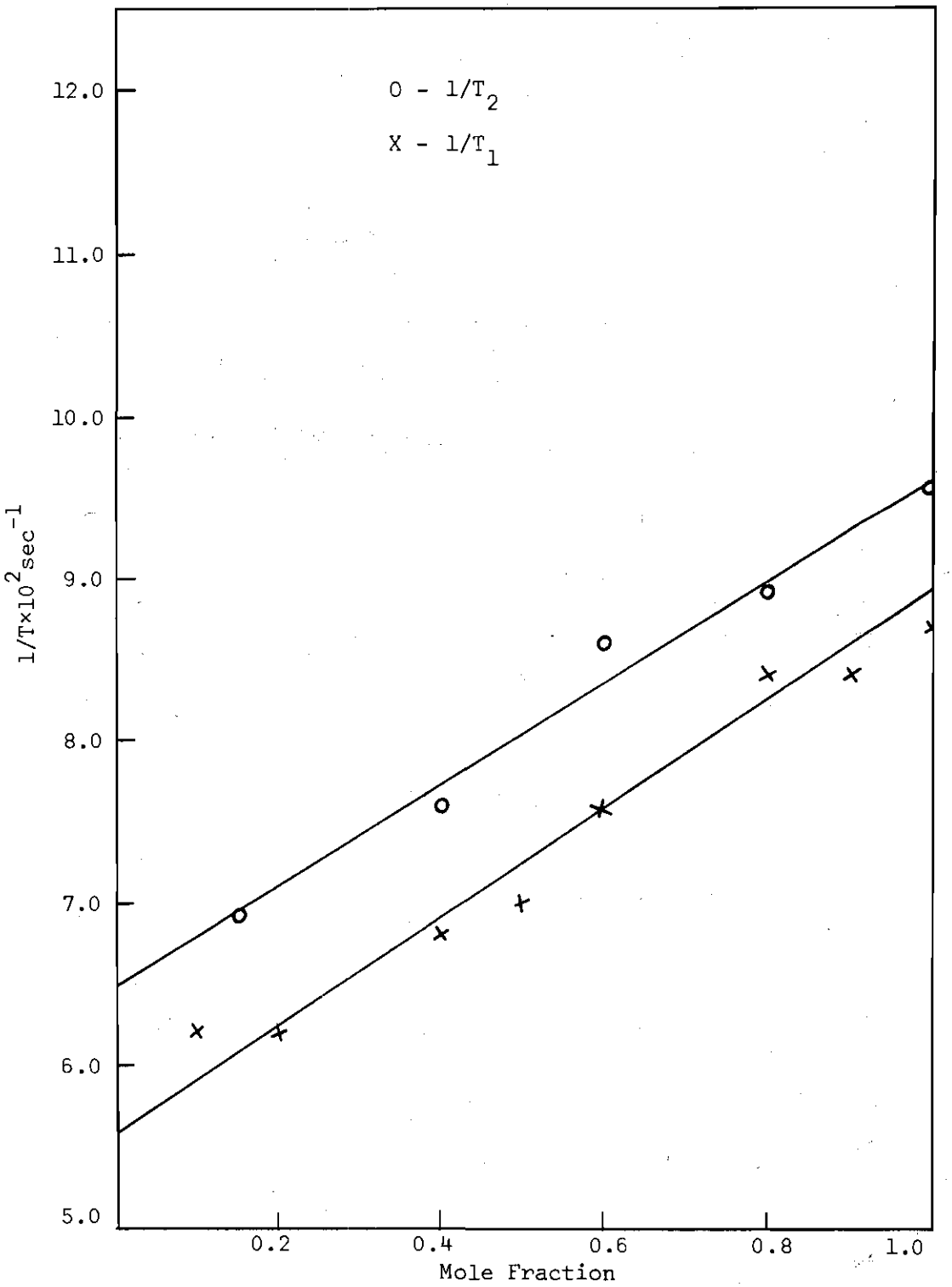

Figure 11. 1,2-Dichloroethane in d_4-1,2-Dichloroethane

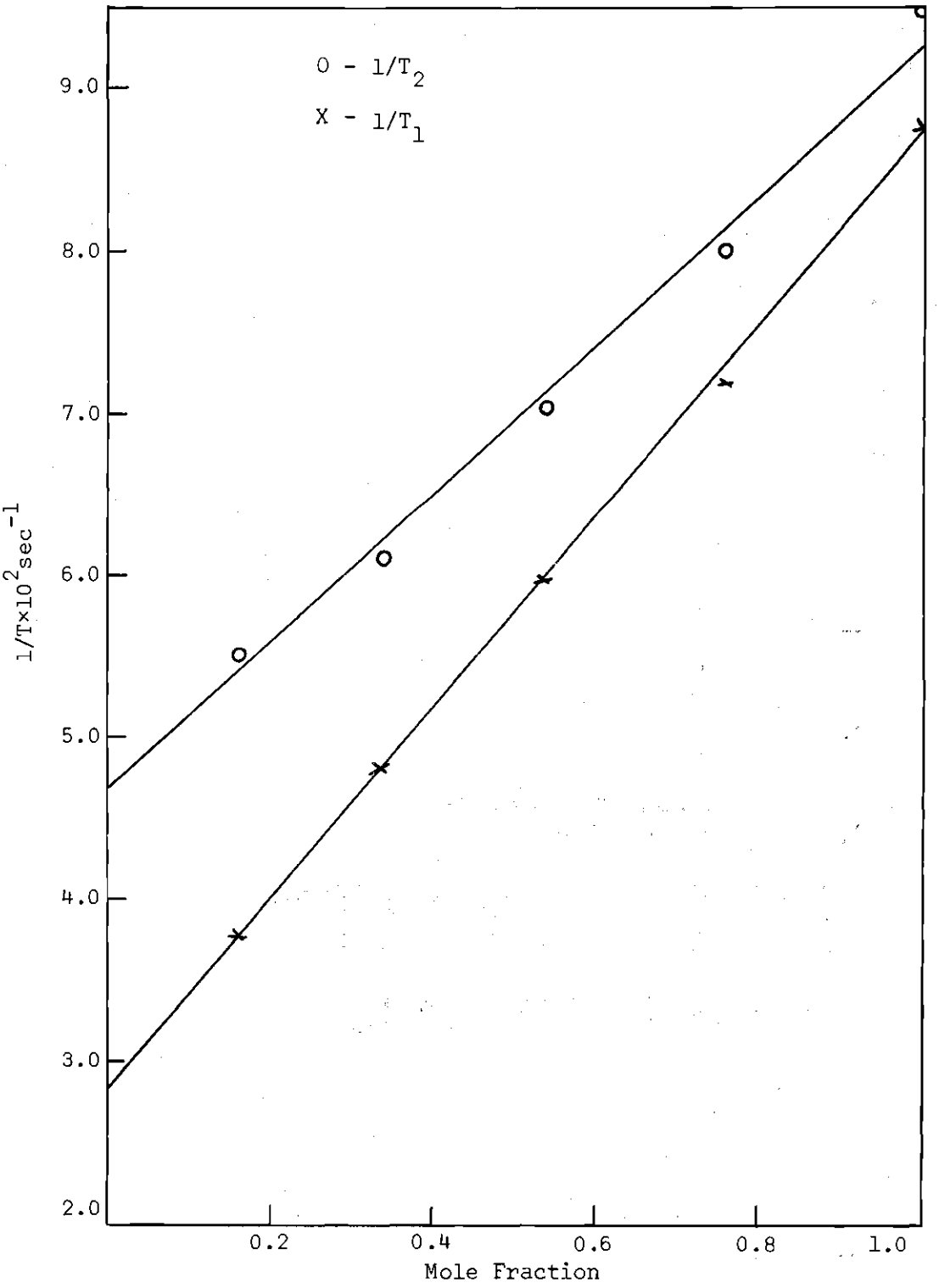

Figure 12. 1,2-Dichloroethane in CS_2

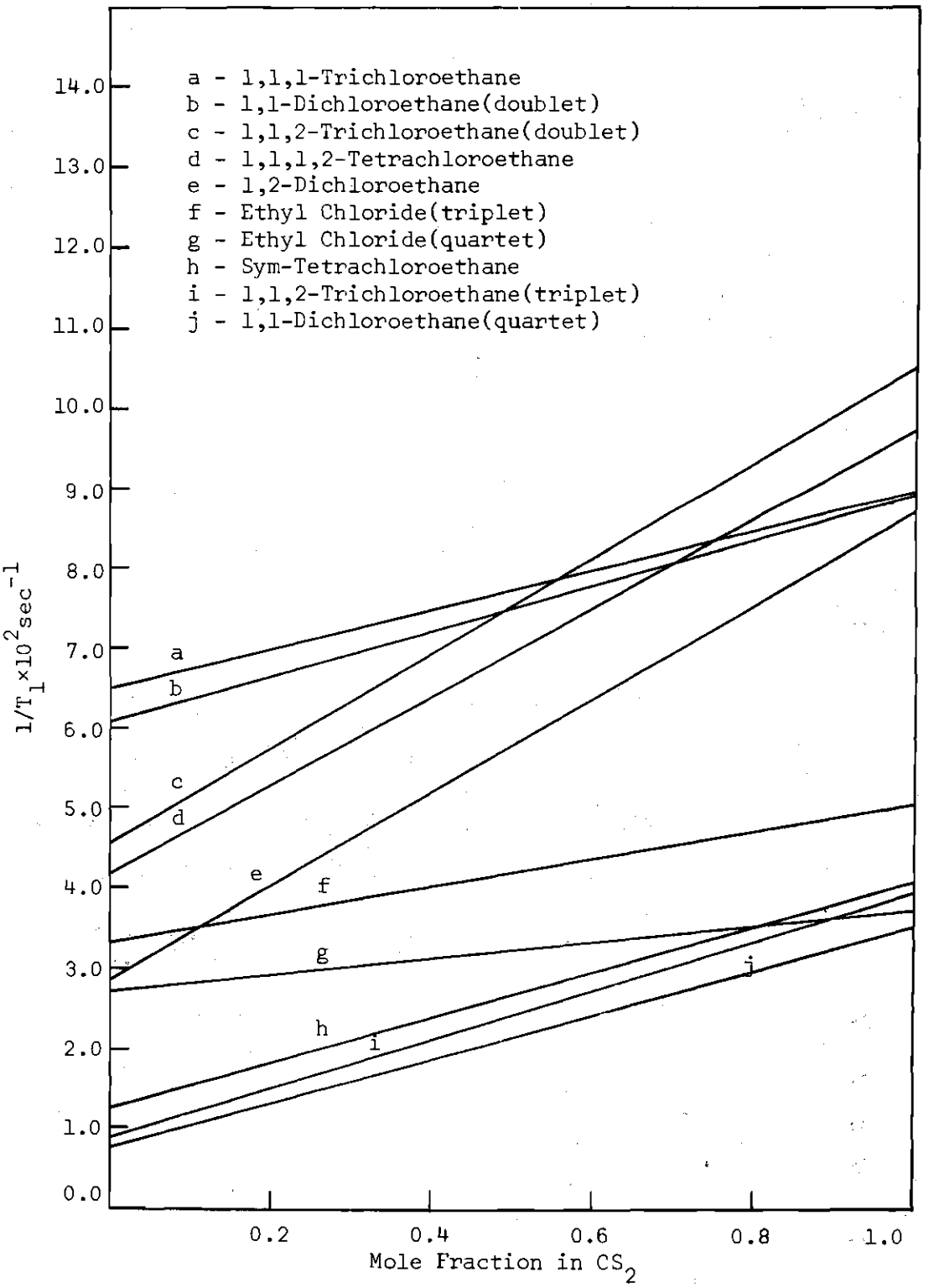

Figure 13. $1/T_1$ as a Function of Mole Fraction Chloroethane in CS_2

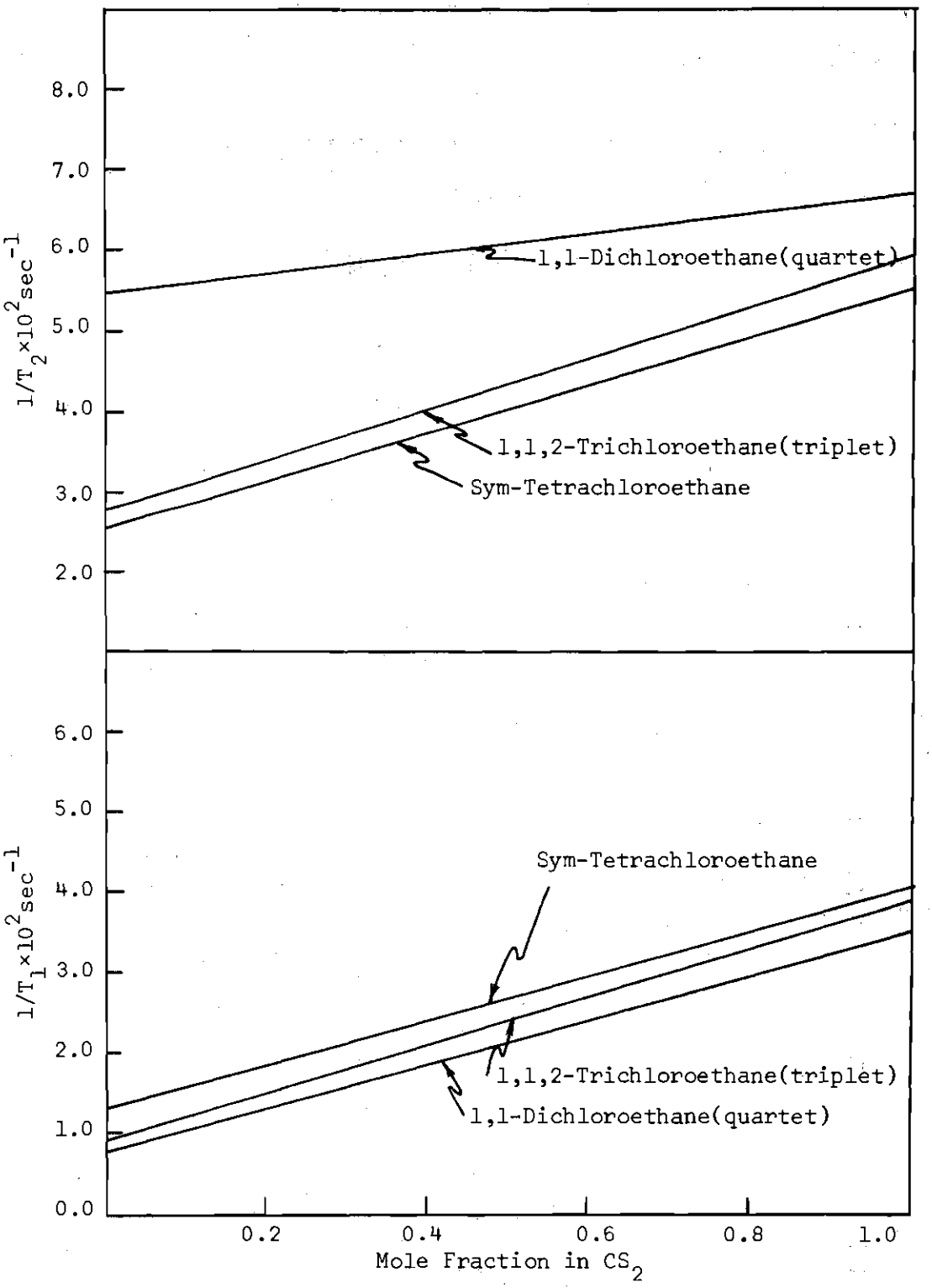

Figure 14. Concentration Dependence of $CHCl_2$ Type Protons

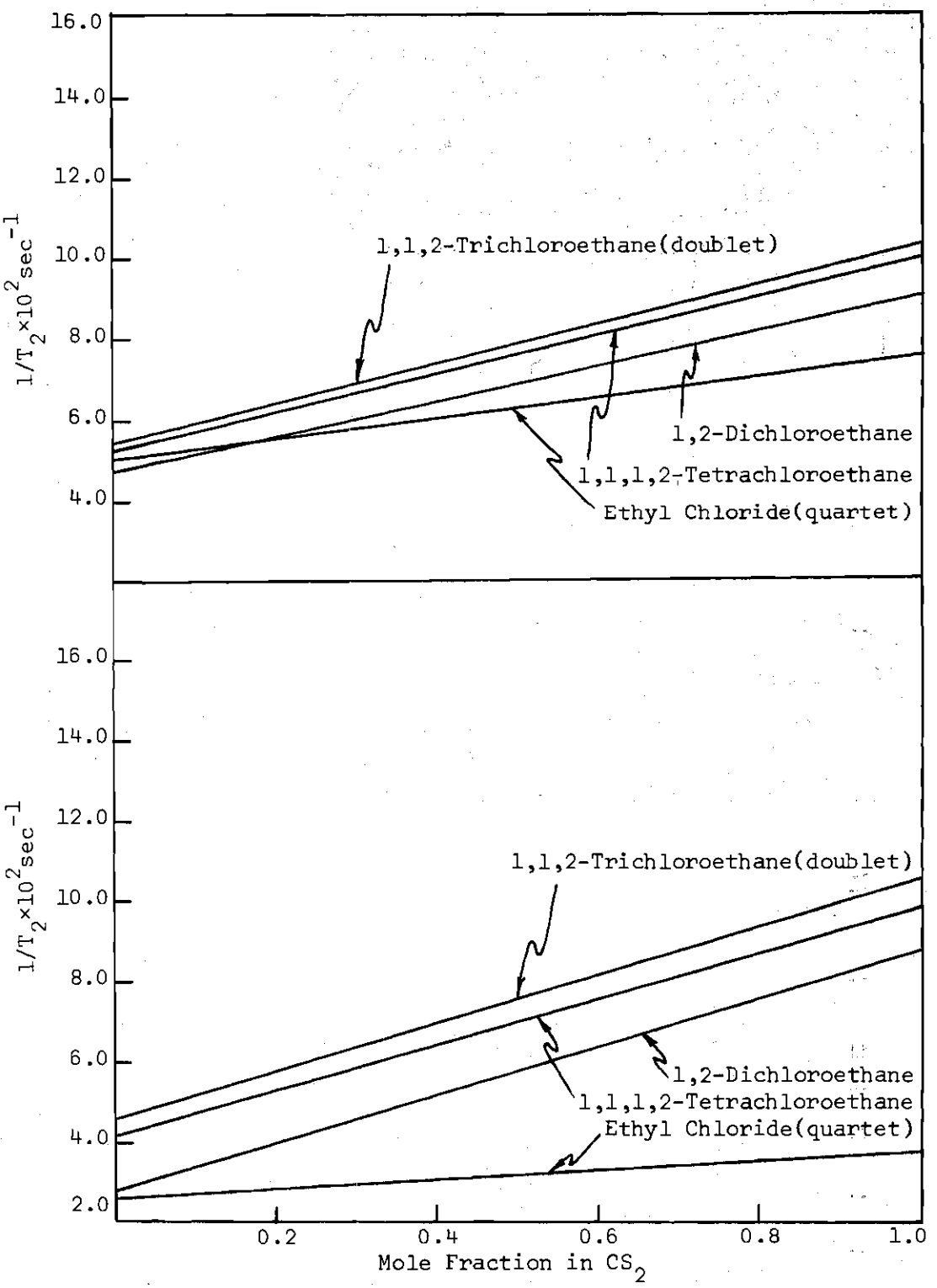

Figure 15. Concentration Dependence of CH_2Cl Type Protons

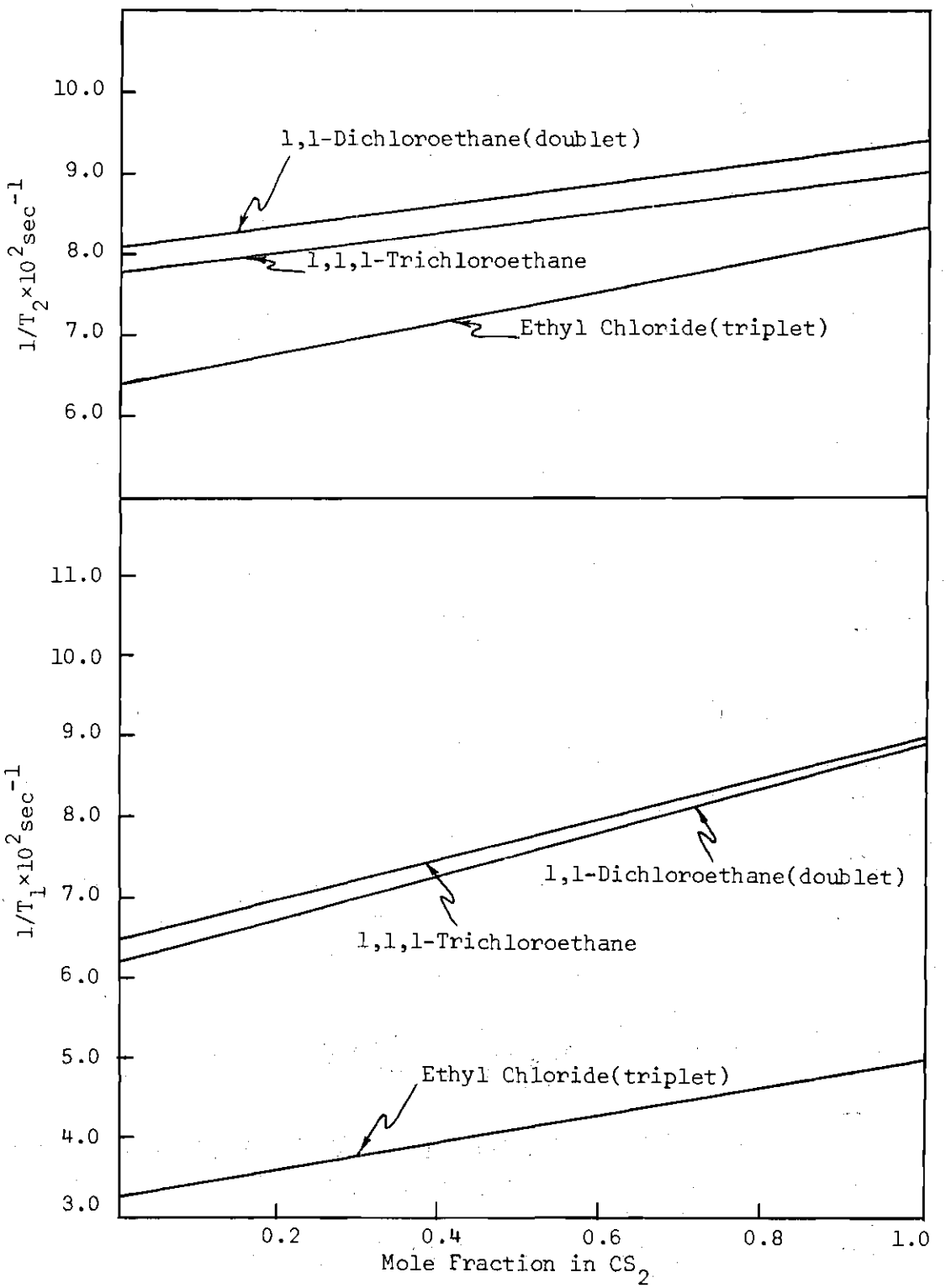

Figure 16. Concentration Dependence of CH_3 Type Protons

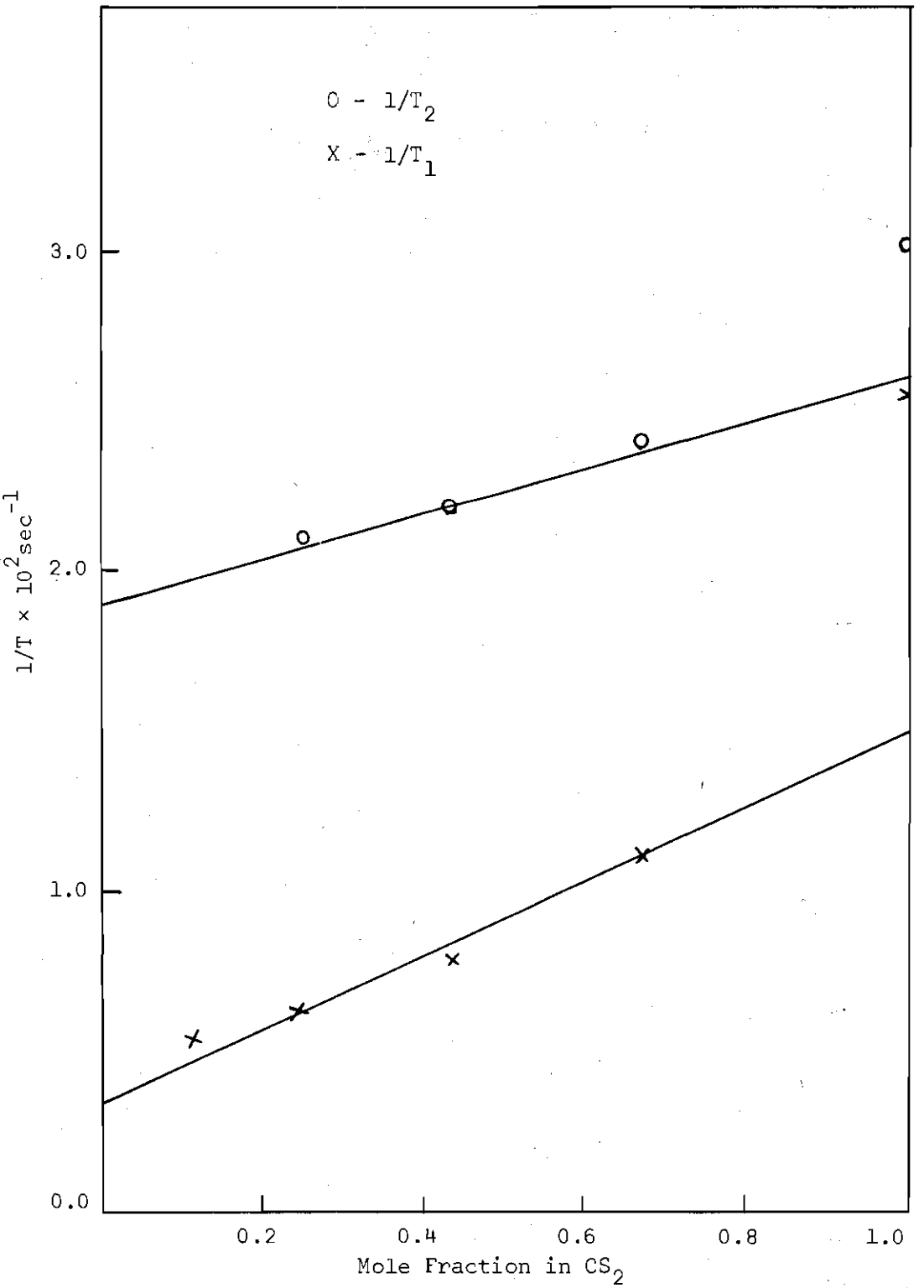

Figure 17. Pentachloroethane in CS_2

measurements were used only for comparison of the experiments; the dilution plots were constructed from the A-60D data. The error limits in Tables 1 and 2 refer to the average deviation of three measurements.

The 1,1-dichloroethane(quartet) and 1,1,2-trichloroethane (triplet) were measured on the DP-60. Because the T_1's for these lines are longer than 40 sec, this was the only method available. Some shorter T_1's were measured with the DP-60 so that a comparison between A-60D and DP-60 methods could be made. Examination of the data in Tables 1 and 2 indicates excellent agreement between these experimental techniques, i.e., less than 10 per cent deviation in most cases.

One possible source of error in comparing experiments on the A-60D and DP-60 is the difference in probe operating temperatures. The operating temperatures of the DP-60 and A-60D probes are 28C° and 34C°, respectively. The viscosity of the sample changes very little over this temperature range, hence the variation in T_1 is negligible. For the purpose of calculating T_1's, an average sample temperature of 31C° is used.

1,2-Dichloroethane Study

The data for 1,2-dichloroethane will be discussed first in order to point out the main features of the relaxation results. Equation (36) predicts that $(1/T_1)_{inter}$ should decrease as the concentration of protons decreases. This prediction can be tested by carrying out the dilution in the fully deuterated analogue of the material under examination. Dilution with the deuterated material does not appreciably alter the molecular environment, hence the correlation times do not change. The

only change is the substitution of protons for deuterons. The magnetic moment of the deuteron is small and inconsequential in contributing to relaxation. The result of such an experiment is shown by the top curve in Figure 9. As the mole fraction of ordinary material is reduced $1/T_1$ decreases as expected. The intercept on the ordinate corresponds to the intramolecular contribution to $1/T_1$, i.e., $(1/T_1)_{intra}$.

The lower curve in Figure 9 represents the same type experiment except with CS_2 as the solvent. In CS_2, the environment about a single 1,2-dichloroethane molecule changes as the dilution proceeds. The result is that the correlation times for both the rotational and translational motion change in addition to the change in the number of proton magnetic moments. Since $1/T_1$ is proportional to the correlation time, the greater slope of the dilution curve in CS_2 indicates that the correlation times are decreasing as the solution becomes more dilute. This is not surprising since the 1,2-dichloroethane molecules are being replaced by the smaller CS_2 molecules. It is to be expected that the remaining 1,2-dichloroethane molecules would move with less restriction.

From Figure 9, $(1/T_1)_{intra}$ for 1,2-dichloroethane is less with CS_2 as the solvent than when d_4-1,2-dichloroethane is the solvent. Therefore, the correlation time must be less in the CS_2 than in the deuterated solvent. This knowledge about the correlation times can be readily applied to a statement about the relative motion of the 1,2-dichloroethane molecule in the two solvents. The correlation times indicate a less restricted motion of the 1,2-dichloroethane molecule when it is surrounded by CS_2 molecules than when its neighbors are other 1,2-dichloroethanes.

From Equation (42)

$$1/T_2 = DD + (1/T_2)_{S.C.} \tag{48}$$

where DD is the dipolar coupling contribution to both $1/T_1$ and $1/T_2$. $(1/T_2)_{S.C.}$ is the contribution from scalar coupling to the chlorine. From Equation (40), $(1/T_2)_{S.C.}$ is proportional to the relaxation time of the chlorine. Therefore, a fast motion is associated with a large scalar coupling contribution.

Figure 10 examines the concentration dependence of $1/T_2$ in the d_4-1,2-dichloroethane and CS_2 solvents. Since dilution in the deuterated solvent does not change the correlation times, the slope of the top curve is simply due to a change in the $(1/T_2)_{inter}$ term. As in the case of $(1/T_1)_{inter}$, the change is due to a decrease in the concentration of proton moments. In the CS_2 solvent, the $(1/T_2)_{S.C.}$ term increases and $(1/T_2)_{intra}$ decreases as the concentration decreases. At low concentrations of the ethane, $(1/T_2)_{S.C.}$ becomes an important contribution to the total $1/T_2$. Scalar coupling does not contribute to $1/T_1$. For this reason the slope of $1/T_2$ is less than for $1/T_1$. The $(1/T_2)_{S.C.}$ begins to compensate for the diminishing dipolar contribution to $1/T_2$ at low concentrations. This effect is clearly observable by noting the larger divergence for the $1/T_1$ curves in Figure 9 than for the $1/T_2$ curves in Figure 10.

Figure 11 is a comparison of the effect of dilution on $1/T_1$ and $1/T_2$ in the deuterated solvent. The only change that occurs is with

the intermolecular interaction. Since the intermolecular interaction affects both $1/T_1$ and $1/T_2$ the same, identical behavior on dilution is expected. The fact that the curves in Figure 11 are parallel substantiates this prediction. The difference between the two parallel lines equals $(1/T_2)_{S.C.}$.

The purpose of extrapolating the relaxation curves to infinite dilution is to remove the intermolecular contribution to $1/T_1$ and $1/T_2$. The intercept on the ordinate of the $1/T_2$ plot is $(1/T_2)_{intra} + (1/T_2)_{S.C.}$. Therefore, the difference between the ordinate intercepts is $(1/T_2)_{S.C.}$. Using previous arguments, the scalar coupling contribution should be less in the deuterated solvent than in CS_2. From Figure 11, the $(1/T_2)_{S.C.}$ is 0.9×10^{-2} sec^{-1} in the deuterated solvent. From Figure 12, $(1/T_2)_{S.C.}$ in CS_2 is 1.9×10^{-2} sec^{-1}, which agrees with the prediction. The divergence of the $1/T_1$ and $1/T_2$ curves in Figure 12 is common to the entire series of chlorinated ethanes. The divergence is caused by the increase in $(1/T_2)_{S.C.}$ as the solution becomes more dilute.

Dipolar Interactions

The members of the series of chlorinated ethanes include all possible combinations of protons and chlorines bonded to two carbon atoms with a single bond between the carbons. The pentachloroethane was was studied, but does not readily fit into the remainder of the series because of the lack of intramolecular dipolar interaction. Three members of this series, 1,1,2-trichloroethane, 1,1-dichloroethane, and ethylchloride, possess non-equivalent protons, hence they exhibit two chemically shifted multiplets. The remaining members of the series

contain only equivalent protons and are characterized by one line spectra.

In Table 3 the spectral lines associated with the series of compounds are grouped according to the number and location of the protons responsible for the line. The dipolar interaction between protons diminishes as the sixth power of the interproton distance. Therefore, protons on the same carbon (a distance of 1.8A apart) are more effective in promoting relaxation than protons on an adjacent carbon (a distance of 2.5 or 3.1A apart). The magnitude of the dipolar interaction is essentially determined by the interaction with dipoles on the same carbon. Interactions between protons across the carbon-carbon bond are observable, but small in comparison to the same carbon interactions.

The difference in magnitude between interactions on the same carbon and on adjacent carbons is illustrated in Figure 13. The three lines with the smallest $1/T_1$ are associated with protons on carbons containing no other protons. The middle set of four curves corresponds to a pair of protons on a carbon. The remaining three lines at the top are due to spectral lines associated with three protons on the same carbon. From this data, it is clear that the dipolar interactions on the same carbon are responsible for the dominant contribution to $1/T_1$.

The effect on $1/T_1$ brought about by changing both the number of dipoles and the correlation time is contained in the expression

$$(1/T_{1i})_{intra} = K\tau \sum_j d_{ij}^{-6} \qquad (49)$$

Table 3. Location of Protons Responsible for Spectral Lines Associated with Series of Chlorinated Ethanes

Spectral Line	Number of Protons on Carbon Under Consideration	Number of Protons on Adjacent Carbon
Penta Chloroethane	1	0
Sym-Tetrachloroethane	1	1
1,1,2-Trichloroethane(Triplet)	1	2
1,1-Dichloroethane(Quartet)	1	3
1,1,2-Trichloroethane(Doublet)	2	0
1,1,1,2-Tetrachloroethane	2	1
1,2-Dichloroethane	2	2
Ethyl Chloride(Quartet)	2	3
1,1,1-Trichloroethane	3	0
1,1-Dichloroethane(Doublet)	3	1
Ethyl Chloride(Triplet)	3	2

K is a constant containing the collection of constants in Equation (32), τ is the rotational correlation time, and d_{ij} is the interproton distance. The addition of protons will increase the value of the summation and in turn increase $(1/T_1)_{intra}$. On the other hand, the addition of protons will cause a decrease in the correlation time, leading to a decrease in $(1/T_1)_{intra}$. It is important to note that the effects oppose each other.

Contributions to $K \sum_j d_{ij}^{-6}$ from various interactions are shown in Table 4.

Table 4. Interatomic Distances Associated with Rotational Isomers

Atoms	$\begin{pmatrix}\text{Interatomic} \\ \text{Distance}\end{pmatrix}$A	$(d^{-6}\times 10^{2})A^{-6}$	$(Kd^{-6}\times 10^{-10})sec^{-2}$
H-H(Same Carbon)	1.80	2.98	2.54
H-H(Gauche)	2.51	0.40	0.34
H-H(Trans)	3.08	0.12	0.10
H-Cl(Same Carbon)	2.38	0.54	0.003
H-Cl(Gauche)	2.91	0.17	0.001
H-Cl(Trans)	3.70	0.04	0.000

Interatomic distances are calculated by assuming a tetrahedral geometry about each carbon and a staggered methyl group configuration (20). The chlorine-proton interactions are seen to be negligible. The CC, CH, and CCl bond distances were assumed to be 1.55A, 1.10A, and 1.78A, respectively.

Energy differences between rotational isomers, and the potential barriers separating the isomers have been determined (21). The preferred rotational confirmations were used in calculating $K \sum_j d_{ij}^{-6}$ in Table 5. $K \sum_j d_{ij}^{-6}$ is proportional to the magnitude of the dipolar interactions and is referred to as the geometrical factor. In cases where both the gauch and trans isomers were equally likely, an average was used. These cases are indicated by (av) in Table 5.

Table 5. Comparison of B.P.P. and Steel Models with Experimental Data

Spectral Line	(Geom$\times 10^{-10}$)sec^{-2}	[τ(diffusion)$\times 10^{12}$]sec	$(1/T_1)_{B.P.P.}$ sec^{-1}	[τ(Steel)$\times 10^{13}$]sec	$(1/T_1)_{Steel}$ sec^{-1}	$(1/T_1)_{Exp}$ sec^{-1}
$CHCl_2$						
1,1-Dichloroethane(quartet)	0.78	12.4	0.10	6.38	0.005	0.008
1,1,2-Trichloroethane(triplet)	0.44	13.9	0.06	8.83	0.004	0.010
Sym-Tetrachloroethane	0.10(S)	15.4	0.02	11.22	0.001	0.013
	0.34(A)		0.05		0.004	
CH_2Cl						
1,2-Dichloroethane	2.98	11.6	0.35	4.92	0.012	.030
1,1,2-Trichloroethane(doublet)(av)	2.76	13.9	0.38	8.83	0.024	.046
1,1,1,2-Tetrachloroethane	2.54	15.8	0.40	10.92	0.028	.042
Ethyl Chloride(quartet)	3.36	10.5	0.35	4.10	0.014	.028
CH_3						
1,1-Dichloroethane(doublet)(av)	5.34	12.4	0.66	6.38	0.034	0.062
1,1,1-Trichloroethane	5.08	15.0	0.76	8.74	0.044	0.065
Ethyl Chloride(triplet)(av)	5.60	10.5	0.59	4.10	0.023	0.033
CCl_3						
Pentachloroethane	0.008	17.7	0.001	12.93	0.0001	0.004

Two methods are available for calculating the correlation time. Bloembergen, Purcell, and Pound (4) have assumed that the molecular rate of reorientation in liquids is controlled by the viscosity of the medium and the volume of the molecule. Debye's model of isotropic rotational diffusion was used to calculate the correlation time, Equation (33). Values for the molecular radius were calculated by assuming that the molecules are spherical and using density data (3). The viscosity is the viscosity of CS_2 at 31C°, and is equal to 0.353 centipoise (26). The temperature, 31C°, is chosen to be representative of the operating temperatures of the A-60D and DP-60 probes. Correlation times calculated from this model are shown in Table 5 under τ (diffusion). The product of τ and Geom. is $(1/T_1)_{intra}$ and is shown in Table 5 as $(1/T_1)_{B.P.P.}$. Values calculated by the B.P.P. theory are usually larger than the observed values by a factor of ten. In other words, the isotropic diffusion relaxation process is too efficient.

An alternative method of calculating the correlation time was proposed by Steel *et al.* (3). Steel assumed that the molecular rotation rate was determined by the moment of inertia of the molecule. Steel gives the expression for the rotational correlation time of a spherical top as (3)

$$\tau(\text{Steel}) = 1/2(\pi I/3kT)^{1/2}. \qquad (50)$$

where I is the moment of inertia. The chlorinated molecules are asymmetric tops, and Equation (50) was used by replacing I by an average

moment of inertia $\bar{I}$ defined by

$$\bar{I}^{-1} = \frac{1}{3}(I_A^{-1} + I_B^{-1} + I_C^{-1}) \qquad (51)$$

where I_A, I_B, I_C are the principal moments of inertia. The principal moments of inertia were calculated using a program kindly supplied by J. Q. Williams of the Georgia Institute of Technology School of Physics. The principal moments of inertia and $\bar{I}^{1/2}$ are listed in Table 6. τ(Steel) is found from Equation (50). $(1/T_1)_{Steel}$ is $(1/T_1)_{intra}$, calculated using Steel's model. From Table 5, Steel's model underpredicts $(1/T_1)_{exp}$, i.e., relaxation is more efficient than predicted by Steel's model. In most cases, however, the Steel model is much better for predicting the observed values than the B.P.P. model. Therefore, rotational motion of the molecules is determined essentially by the moment of inertia rather than by the viscosity of the medium.

In the case of sym-tetrachloroethane there is a large difference between the geometrical factors for the symmetric and asymmetric isomers. For this reason they are considered independently. The asymmetric isomer gives good agreement with the Steel model; the symmetric good agreement with the B.P.P. model. The other chloroethanes only agree with the Steel model. Therefore, it seems reasonable to expect that the asymmetric isomer is the dominant isomer in solution.

It was previously learned that dipolar interactions between protons on the same carbon were largely responsible for determining $(1/T_1)_{intra}$. The effect of dipolar interactions across the CC bond

Table 6. Moments of Inertia

Compound	$\times 10^{40}$ gm cm^2 I_A	I_B	I_C	$(\bar{I}^{1/2} \times 10^{20})$ gm$^{1/2}$ cm
CH_3CH_3	10.8	42.4	42.4	4.63
CH_3CH_2Cl	46.1	152	169	9.39
$CHCl_2CH_3$	133	264	372	14.6
CH_2ClCH_2Cl(sym)	29.3	568	587	8.9
(asym)	93	341	407	13.6
CH_3CCl_3	361	361	503	20.0
$CHCl_2CH_2Cl$(asym)	227	580	780	20.1
(sym)	315	415	602	20.3
CCl_3CH_2Cl	444	762	820	25.0
$CHCl_2CHCl_2$(sym)	511	639	1122	26.1
(asym)	456	728	885	25.3
CCl_3CHCl_2	729	864	1130	29.6
CCl_3CCl_3	995	1183	1183	33.4

is much less. The first three spectral lines in Figure 5 are associated with a $CHCl_2$ group. The three lines differ in the number of protons on the carbon adjacent the $CHCl_2$ group. If dipolar interactions across the CC bond were determining $(1/T_1)_{intra}$, $(1/T_1)_{exp}$ would increase as protons were added to the adjacent carbon. $(1/T_1)_{exp}$ actually decreases as protons are added. The effect of adding protons is to decrease the

moment of inertia, hence the correlation time and $1/T_1$. Although, the dipolar interactions are increased by the addition of protons, the decreased correlation time more than compensates for the increased dipolar interaction. Table 5 shows excellent agreement between the moment of inertia, ($\bar{I}$), and $(1/T_1)_{exp}$. In almost all cases, an increase in $\bar{I}$ is accompanied by an increase in $1/T_1$. The only exception is between 1,1,1,2-tetrachloroethane and 1,1,2-trichloroethane(doublet). As $\bar{I}$ increases, $(1/T_1)_{exp}$ decreases. The explanation is that the additional dipolar interaction in the trichloroethane(doublet) is more important than the decrease in correlation time.

The possibility of internal molecular motions contributing to relaxation must be considered. Torsional frequencies and barriers to rotation are given in reference (21). The torsional frequencies are of the order of 10^{12} cps or two orders of magnitude larger than the rotational transition frequencies. Collisions will not be effective in inducing torsional transitions, hence torsional motions would not be expected to contribute to relaxation. Using the potential barriers to internal rotation from reference (21) and the expression for the absolute rate constant (22), a correlation time for internal rotation was calculated. Ethane was found to have the smallest correlation time, $\tau = 2\times10^{-11}$sec. Hexachloroethane had the largest, $\tau = 3\times10^{-6}$sec. For internal rotation to be important, its correlation time would have to be similar to that for ethane. Those molecules with chlorines on only one carbon are similar to ethane in that they have the smallest potential barriers and the shortest correlation times. Therefore, the mole-

cules, 1,1,1-trichloroethane, 1,1-dichloroethane and ethyl chloride, are most likely to receive contributions from internal molecular rotation.

In Figure 14, the $1/T_2$ curve for 1,1-dichloroethane(quartet) is out of line with the other two members of the series. This may be due to internal rotation making an additional contribution to $(1/T_2)_{S.C.}$. The proton responsible for the quartet is on a carbon with two chlorine atoms. Therefore, scalar coupling might be expected to make a contribution to $1/T_2$.

The proton on pentachloroethane is unique in that there are no other protons on the molecule by which it can be relaxed. From Figure 17, the $(1/T_1)_{intra}$ is 0.004 Sec^{-1} which is small in comparison to situations where there are other proton magnetic moments available. One possibility for this intramolecular contribution is the dipolar interaction with the chlorine magnetic moment. From the B.P.P. model, the intramolecular contribution from the chlorine magnetic moments is found to be 0.001 sec^{-1}. This is in fair agreement with the experimental value.

Scalar Coupling

From Equation (41), $(1/T_2)_{S.C.}$ is proportional to the chlorine relaxation time. The chlorine relaxation is due to the interaction of the chlorine nuclear quadrupole moment with fluctuating electric field gradients and is given by the expression (15)

$$1/T_{Cl} = (1/20)e^4\pi^2Z^2Q^2\tau_c \qquad (52)$$

where eq is the electric field gradient, and eQ is the nuclear quadrupole moment. τ_c is the rotational correlation time as occurs in the intramolecular dipolar mechanism. From Equation (6) and Equation (41), $(1/T_2)_{S.C.}$ is inversely proportional to the rotational correlation time. This is in contrast to $(1/T_1)_{intra}$ which is proportional to the correlation time.

The electric field gradients along the CCl bonds are approximately the same for all CCl bonds in all of the ethanes. This is probably true to about 15 per cent, as can be seen from data on the chlorinated methanes (23), and ethyl chloride (24). Therefore, changes in $(1/T_2)_{S.C.}$ can be expected to reflect changes in the number of chlorines and the rotational correlation time. An increase in the number of chlorines should increase $(1/T_2)_{S.C.}$. An increase in correlation time should cause a decrease in $(1/T_2)_{S.C.}$ and an increase in $(1/T_1)_{intra}$.

The spectral lines in Figure 14 are associated with a $CHCl_2$ type proton. The adjacent carbon may contain either 1, 2, or 3 protons. $(1/T_2)_{S.C.}$ is given in Table 7 along with $(1/T_1)_{intra}$. As $(1/T_2)_{S.C.}$ increases from 1.3 sec^{-1} to 4.7 sec^{-1}, $(1/T_1)_{intra}$ decreases from 1.3 sec^{-1} to 0.8 sec^{-1}. The increase in $(1/T_2)_{S.C.}$ is due to a decrease in rotational correlation time, which causes a corresponding decrease in $(1/T_1)_{intra}$. Figure 15 contains data for lines associated with a CH_2Cl type proton. Figure 16 data refers to a CH_3 type proton. The $(1/T_2)_{S.C.}$ contribution is given in Table 7.

Table 7. Comparison of Scalar Coupling and Intramolecular Interactions

Spectral Lines	$\left(\frac{1}{T_2}\right)_{S.C.} \times 10^2 sec^{-1}$	$\left(\frac{1}{T_1}\right)_{Intra} \times 10^2 sec^{-1}$
Sym-Tetrachloroethane	1.3	1.3
1,1,2-Trichloroethane(Triplet)	1.9	1.0
1,1-Dichloroethane(Quartet)	4.7	0.8
1,1,2-Trichloroethane(Doublet)	0.7	4.6
1,1,1,2-Tetrachloroethane	1.0	4.2
1,2-Dichloroethane	1.8	3.0
Ethyl Chloride(Quartet)	2.9	2.8
1,1,1-Trichloroethane	1.2	6.5
1,1-Dichloroethane(Doublet)	1.9	6.2
Ethyl Chloride(Triplet)	3.3	3.3

Within each group, $(1/T_2)_{S.C.}$ increases a $(1/T_1)_{intra}$ decreases. This is consistent with changes in correlation times suggested by the $1/T_1$ data.

BIBLIOGRAPHY*

1. B. H. Muller, and N. Noble, *J. Chem. Phys. 38,* 777 (1963).

2. G. Bonera, L. Chiodi, G. Lanzi, and A. Rigamonti, *Nuovo Cimento, Vol. XVII, No. 2,* 198 (1960).

3. W. Moniz, W. Steel, and J. Dixon, *J. Chem. Phys., 38,* 2418 (1963).

4. N. Bloembergen, E. Purcell, and R. V. Pound, *Phys. Rev., 73,* 679 (1948).

5. A. Abragam, and R. V. Pound, *Phys. Rev., 92,* 943 (1953).

6. A. Carrington, and A. D. McLachlan, *Introduction to Magnetic Resonance,* Harper and Row, New York, 1967.

7. A. Abragam, *The Principles of Nuclear Magnetism,* Oxford University Press, London, 1961.

8. P. Debye, *Polar Molecules,* Dover Publications, New York, 1945.

9. J. Pople, W. Schneider, and H. Bernstein, *High-Resolution Nuclear Magnetic Resonance,* McGraw-Hill, New York (1959).

10. H. S. Gutowsky, and D. E. Woessner, *Phys. Rev., 104,* 843 (1956).

11. N. Ramsey, *Nuclear Moments,* John Wiley Inc., New York, 1953.

12. J. G. Powles, and D. K. Green, *Phys. Letters, 3,* 134 (1962).

13. G. Bonera, I. Chiodi, L. Giulotto, and G. Lanzi, *Nuovo Cimento, Vol. XIV, No. 1,* 520 (1959).

14. D. E. Drain, *Phys. Soc. London, 62A,* 301 (1949).

15. S. Meiboom, *J. Chem. Phys., 34,* 375 (1961).

16. J. H. Noggle, *Rev. Sci. Instr., 35,* 1495 (1964).

---

*Journal title abbreviations used are those listed in "Index of Periodicals," *Chemical Abstracts,* 1961.

17. E. L. Hahn, *Phys. Rev.*, *77*, 297 (1950).

18. H. Carr, and E. Purcell, *Phys. Rev.*, *94*, 630 (1954).

19. S. Meiboom, and D. Gill, *Rev. Sci. Instr.*, *29*, 688 (1958).

20. Tables of Interatomic Distance and Configuration in Molecules and Ions, Chem. Soc. London, Special Publications, *No. 11* (1958).

21. G. Geoffrey, P. Brier, and G. Lane, *Trans. Faraday Soc.*, *63*, 824 (1967).

22. S. Glasstone, K. Laidler, and H. Eyring, *The Theory of Rate Processes*, McGraw-Hill Inc., N. Y., 1961.

23. P. Wolfe, *J. Chem. Phys.*, *25*, 976 (1956).

24. R. Schwendeman, and G. Jacobs, *J. Chem. Phys.*, *36*, 1245 (1962).

25. Varian Associates, *NMR and EPR Spectroscopy*, Pergamon Press, New York, 1960.

26. The Chemical Rubber Co., *Handbook of Chemistry and Physics, 44th Edition*, The Chemical Rubber Publishing Company, Ohio, 1963.

VITA

Charles R. Miller was born November 25, 1941, in Kingston, Pennsylvania. Upon graduation from high school, he enlisted in the U. S. Air Force. He completed a four-year tour of active military service, and received an honorable discharge. In 1962, he entered Centenary College, Shreveport, Louisiana, and graduated with a B. S. degree in Chemistry in June of 1965.

In September, 1965, he was appointed a Graduate Teaching Assistant in the School of Chemistry at the Georgia Institute of Technology, Atlanta, Georgia. In September, 1966, he was appointed Research Assistant in the School of Chemistry at Georgia Tech and served in that capacity until March, 1970.